Fish debris in sediments from the last 25 kyr in the Humboldt Current reveal the role of productivity and oxygen on small pelagic fishes

Renato Salvatteci, Dimitri Gutiérrez, David Field, Abdel Sifeddine, Luc Ortlieb, Sandrine Caquineau, Tim R. Baumgartner, Vicente Ferreira, Arnaud Bertrand

Progress in Oceanography
May 2019, Volume 176, Pages 102114 (26p.)
https://doi.org/10.1016/j.pocean.2019.05.006
https://archimer.ifremer.fr/doc/00500/61147/

Fish debris in sediments from the last 25 kyr in the Humboldt Current reveal the role of productivity and oxygen on small pelagic fishes

Salvatteci R. [1, *], Gutierrez D. [2, 3], Field D. [4], Sifeddine A. [5, 6], Ortlieb L. [5], Caquineau S. [5], Baumgartner T. [7], Ferreira V. [7], Bertrand Arnaud [8]

[1] Institute of Geosciences, Kiel University, Kiel, Germany
[2] Instituto del Mar del Perú (IMARPE), Esquina Gamarra y General Valle s/n, Callao, Perú
[3] Programa de Maestría de Ciencias del Mar, Facultad de Ciencias y Filosofía, Universidad Peruana Cayetano Heredia, Lima, Perú
[4] College of Natural Sciences, Hawaii Pacific, University, Kaneohe, HI, USA
[5] Institut de Recherche pour le Développement (IRD, Sorbonne Université, CNRS, MNHN), LOCEAN Laboratory, Bondy, France
[6] Departamento de Geoquímica, LMI PALEOTRACES (IRD, UPMC, UFF, Uantof, UPCH), Universidade Federal Fluminense, Niteroi, RJ, Brazil
[7] Centro de Investigación Científica y de Educación Superior de Ensenada, Ensenada, Baja California C.P, México
[8] IRD, MARBEC, Univ Montpellier, CNRS, Ifremer, IRD, Sète, France

* Corresponding author : R. Salvatteci, email address : renatosalvatteci@gmail.com

Abstract :

Upwelling of cold, nutrient-rich water from the oxygen minimum zone (OMZ) off Peru sustains the world's highest production of forage fish, mostly composed of anchovy (Engraulis ringens). However, the potential impacts of climate change on upwelling dynamics and thus fish productivity in the near future are uncertain. Here, we reconstruct past changes in fish populations during the last 25,000 years to unravel their response to changes in OMZ intensity and productivity. We quantified and identified fish scales and bones deposited in laminated sediments from Pisco (Peru) with an average sampling resolution of 20.4 years (±7.1). The records span the Last Glacial Maximum to the recent Holocene and thus encompass a variety of combinations of productivity, oxygen, and global temperature. Our results reveal that productivity appears to be the main factor controlling small pelagic fish abundance, while sub-surface oxygenation affects mainly anchovy and likely sardine populations. Lower productivity and higher oxygen concentrations during the glacial resulted in lower total fish productivity, whereas higher productivity and a stronger OMZ in some time intervals during the Holocene resulted in higher fish abundances. A variety of different conditions between these two oceanographic end members indicate preferred environmental conditions for a variety of small pelagic fishes. There is no evidence in our record for an out of phase relationship between anchovy and sardine at the timescales examined in the present study. Anchovy have been the predominant small pelagic fish throughout the record, at least over centennial to millennial timescales. Its abundance reached a maximum during the Current Warm Period, an era characterized by high productivity and intense OMZ conditions. Thus, industrial fisheries developed during a period of exceptional productivity in relation to that of the last 25 kyr. The records reveal that dramatic decreases

in pelagic fish abundances have occurred in response to past large-scale climate changes than those observed in the instrumental period, which suggests that future climate change may result in substantial changes in ecosystem structure.

Highlights

► Anchovy and other fishes fluctuated from multidecadal to millennial timescales. ► Productivity appears as the main factor controlling small pelagic fish abundance. ► Sub-surface oxygenation seems to play a role in a species-dependent way. ► The industrial fishery developed during a period of exceptional fish productivity.

1. Introduction

In Eastern Boundary Upwelling systems (EBUS), coastal upwelling results from alongshore winds generating an offshore Ekman drift, which produces a pumping of cool and nutrient-rich waters fueling high productivity (Chavez and Messié, 2009). The Humboldt Current System (HCS) is notable for its outstanding anchovy (*Engraulis ringens*) production (Chavez et al., 2008). The northern HCS off Peru presently produces more fish per unit area than any other region in the oceans; it represents 0.1% of the world ocean but can produce up to 10% of the world fish catch (Chavez et al., 2008). However, small pelagic fishes are characterized by marked fluctuations in their stock size on interannual to multidecadal timescales due to environmentally-driven changes in recruitment (Bertrand et al., 2004; Barange et al., 2009). Analyses of fish scales from sediment cores have consistently shown that large variability in population sizes occurs on decadal to multidecadal timescales that may be caused by changes in regional and/or large-scale ocean/atmosphere coupling of the last several hundred or last several thousand years (Baumgartner et al. 1992; Gutiérrez et al., 2009; Kuwae et al., 2017; Salvatteci et al., 2018). Still, the response of pelagic fish populations to climate changes on millennial and longer timescales, when glacial/interglacial changes result in major reorganizations in

productivity, oxygen, and temperature across the ocean, are poorly known (De Vries and Pearcy, 1982; Sibert et al., 2014; Sibert and Norris, 2015). However, analysing changes in fish populations across such events would likely indicate some of the more important driving mechanics of change.

Several unique circumstances are necessary to have laminated sediments that preserve fish scales, thus yielding long-term records of population variability before the start of the industrial fishery that provide unique insights to understand the relationships between climate change and fish abundance (Soutar and Isaacs, 1974; Baumgartner et al., 1992; Field et al., 2009; Finney et al., 2010; Salvatteci et al., 2018). Over time, fish scales and other types of fish debris fall to the ocean floor, bury and accumulate. Variation in fish scale deposition with fish population size is attributable to natural scale shedding (Field et al., 2009). Low bottom-water oxygenation and high sedimentation rates, characteristics typical of the Pacific's EBUS, are required to preserve records that provide a history of the pelagic fish populations that inhabited the area. Fish debris records from several sites around the world revealed the response of fish populations to past climate changes (Soutar and Isaacs, 1974; De Vries and Percy 1982; Baumgartner et al., 1992; O'Connell and Tunnicliffe, 2001; Díaz-Ochoa et al., 2008; Valdés et al., 2008; Gutierrez et al., 2009; Guiñez et al., 2014; Sibert and Norris, 2015; Skrivanek and Hendy, 2015; Cartes et al., 2017; Salvatteci et al., 2018). In particular, the modes and timescales of variability observed in the fish scale records demonstrate that the range of variations observed in the second half of the 20th century represent only part of the multiple responses of the EBUS to climatic and oceanographic changes (Field et al., 2009; Salvatteci et al., 2018)

While DeVries et al. (1982) developed fish scale records for several periods within the Holocene, the response of fish population to climate changes in the HCS during the last ~25 kyr, a time-period that encompassed major climate changes around the globe, are unknown. However, the response of regional conditions to global climate that occurred during the last 25 kyr offer a good mean to test the fish community response to changes in water column deoxygenation and productivity. In the HCS, the OMZ intensity and productivity showed large variations at multidecadal to millennial timescales associated with major global climate shifts

(Rein et al., 2005; Chazen et al., 2009; Doering et al., 2016; Scholz et al., 2014; Salvatteci et al. 2014b; 2016).

The last 25 kyr comprises the Last Glacial Maximum (LGM, 23-19 kyr BP), the Termination 1 (19-11.4 kyr BP) that includes the Heinrich 1 Stadial (H1S, 18-15 kyr BP) and the Antarctic cold reversal (ACR, 14.7 to 12.5 kyr BP), and the Holocene (11.5 kyr BP to the present). During the LGM, time period of the most recent maximum in globally integrated ice volume (Mix et al., 2001), the Eastern Tropical Pacific was cold (Koutavas et al., 2002), the OMZ in the tropical Pacific was weak, and the productivity off Peru was relatively low compared with the Holocene (Salvatteci et al., 2016). During the Termination 1, a warm time period between the LGM and the Holocene, a rapid increase in water column denitrification occurred in the ocean (Jaccard and Galbraith 2012; Jaccard et al., 2014; Salvatteci et al., 2016). An important climate episode during the Termination 1 was the ACR, a cooling episode that interrupted the warming trend that occurred during the Termination 1 period (Pedro et al., 2015). The Holocene is considered a relatively stable period compared with the large changes observed during the LGM and Termination 1, however several works suggest that the Holocene was also marked by strong climatic and oceanographic changes (Mayewski et al., 2004; Carré et al., 2014).

Understanding fish response to these past changes in climate is important since the future of EBUS under climate change is uncertain given that the global increase in temperatures could increase either stratification or upwelling in these regions (Sydeman et al., 2014; Wang et al., 2015). Bakun (1990) proposed that increasing greenhouse gas concentrations would force an intensification of upwelling-favorable winds in the EBUS. Indeed, contrary to most other marine systems, the HCS experienced a cooling associated with an increase in productivity from the start of the 20th century to recent years (Gutierrez et al., 2011; Salvatteci et al., 2018). Most recent studies converge towards an expected increase in the intensity and duration of upwelling-favorable winds in the southern HCS off Chile, and a moderate decrease off Peru (e.g. Belmadani et al., 2014; Wang et al., 2015). Finally, coupled physical-biogeochemical models predict a future reduction in phytoplankton and zooplankton abundances as a result of large-scale nutrient depletion in subsurface water (Brochier et al., 2013). The uncertainty about physical and

biogeochemical processes is even more critical for the future of small pelagic fish population that depend on the complex interactions with climate dynamics (Bertrand et al., 2018).

Another poorly understood issue facing some marine species is how an expansion of oxygen depleted waters will affect populations by reducing inhabitable waters (Prince and Goodyear, 2006; Stramma et al., 2012). Oxygen Minimum zones (OMZ) are places in the ocean where oxygen concentration is very low due to a combination of weak ocean ventilation, which supplies oxygen, and enhanced respiration, which consumes oxygen (Karstensen et al., 2008). Off Peru, the OMZ occurs between 50 and 600 m depth, and minimum oxygen values (<0.1 $ml.l^{-1}$) are reached at 300–400 m depth (Fig. 1A). Time series from the past decades reveal a vertical expansion of the OMZ that may have dramatic consequences for ecosystems and coastal economies (Stramma et al., 2008; Schmidtko et al., 2017; Levin 2018; Breitburg et al., 2018). In the HCS, changes in sub-surface oxygenation and oxycline depth are associated with fluctuations in the abundance and distribution of anchovy and sardine (*Sardinops sagax*) at temporal and spatial scales (Bertrand et al., 2011). During the 1960s-early 1970s and the 1990s-2000s, when oxygen concentration was low and the oxycline shallow, anchovy was abundant but sardine did not proliferate, while the opposite occurred during the late 1970s and 1980s when sardine flourished (Bertrand et al., 2011). Nevertheless, the current OMZ intensity and size is not unprecedented and has strongly varied in the geological past (Scholz et al., 2014; Salvatteci et al., 2016), probably affecting fish populations.

Considering this global context and the uncertain future, here we use proxies for environmental change, which include export production and sub-surface oxygenation, and fish debris preserved in laminated sediments to address the effects of the changes in OMZ intensity and marine productivity on fish populations in the HCS over the last 25 kyr.

2. Environmental Setting

2.1 Study site

The cores used in the present study were retrieved on the upper continental margin off Pisco (~14 ºS), central-southern Peru (Fig. 1). The Pisco area has the most intense alongshore winds in the Peruvian coast (Goubanova et al., 2011). The upwelling off Pisco is active

throughout the year but is stronger during winter and spring, while primary productivity is higher during spring and summer, when surface waters are more stratified (Echevin et al., 2008; Gutierrez et al., 2011). The site lies south of the present nucleus of the northern fishing stock of anchovy, and that of sardine during the 1980s when sardine fully dominated the HCS (Gutiérrez et al., 2012).

2.2 Distribution and habitat of the main fishes leaving remains in sediments off Peru

2.2.1 Anchovy (*Engraulis ringens*)

The Peruvian anchovy is ecologically and economically the most important pelagic fish in the HCS (e.g., Chavez et al., 2008). It is widely distributed along the western coast of South America between 04º30 and 42º30S (Checkley et al., 2009). Historically, two fishing stocks have been recognized off Peru: the north-central stock from northern Peru to ~15ºS and the southern stock, from 15ºS to the southern limit of Peru (Pauly and Tsukayama, 1987; Checkley et al., 2009). The anchovy is considered an r-type species because of its fast growth, time to maturity (1 year) and short life span (~4 years; Froese and Pauly, 2018). It inhabits water above the oxycline (Bertrand et al., 2010, 2011) in recently upwelled cold coastal water (CCW) and other associated cold and productive water masses (Swartzman et al., 2008). The anchovy forages on both phytoplankton (mainly diatoms) and zooplankton, but the euphausiids and copepods are by far the most important component of its diet (Espinoza and Bertrand, 2008). Anchovy is the main prey for several marine mammals, seabirds, fish and fishers (Bertrand et al., 2012; Joo et al., 2014; Barbraud et al., 2018). Anchovy has high plasticity to cope with the high environmental variability in the HCS (Bertrand et al., 2008; Espinoza and Bertrand 2008) and can be bottom-up controlled at multiple timescales (Bertrand et al., 2008; Salvatteci et al., 2018).

2.2.2 Sardine (*Sardinops sagax*)

Sardine is widely distributed along the western coast of South America from Galapagos Islands up to 42ºS (Checkley et al., 2009). Off Peru, an increase in sardine population occurred when the decline of anchovy took place at the beginning of the 1970s, partially supporting the fishery after the anchovy crash. Sardine, like anchovy, is a small pelagic (but larger than anchovy) that inhabits the upper meters of the water column, but, in contrast to anchovy, do not tolerate low oxygen conditions (Bertrand et al., 2011). Sardine tolerates a large range of

temperatures (~9 – 25º) and presents a rather ubiquitous distribution according to water masses (Swartzman et al., 2008). Off Peru, sardine are distributed further offshore than the anchovy, at the border of the intense upwelling zone (Swartzman et al., 2008). As in the case of anchovy, the diet of sardine is based on zooplankton but of smaller size (mainly smaller copepods and fewer euphausiids) and in lesser degree dinoflagellates (Espinoza et al., 2009).

2.2.3 Jack mackerel, chub mackerel and saury

Jack mackerel (*Trachurus murphyi*) is a transboundary species that constitutes one of the most important fishery resource of Peru and Chile. The jack mackerel is a pelagic species that has a long lifespan (16 years) and reaches maturity at a length of 20-30 cm (2-4 years of age; Froese and Pauly, 2018). It has a wide area of distribution, extending across the whole sub-tropical area of the South Pacific Ocean from South America to New Zealand (Gerlotto et al., 2012). The diet of jack mackerel varies with the fish size, the largest jack mackerel (>40 cm) feed on anchovy and other small pelagics, the mid-sized jack mackerels (between 20 and 40 cm) feed on zooplankton (mainly euphausiids), while the smallest feed on copepods (Alegre et al., 2015). Like sardine, jack mackerel distribution and abundance are associated with sub-surface oxygen concentrations over a wide variety of scales; they avoid areas where the oxygenated surface layer over a low oxygen water column is too thin (Bertrand et al., 2016).

Chub mackerel (*Scomber japonicus*) is a cosmopolitan coastal-pelagic species targeted by artisanal and industrial fisheries off Peru. This species inhabits warm and temperate waters of Atlantic, Indian and Pacific Oceans (Castro and Santana, 2000). It has a relatively long lifespan (12 years) and reaches maturity at ~20-30 cm at the age of 3 years (Castro and Santana, 2000). The chub mackerel off Peru consumes more fish than jack mackerel, despite having a smaller maximum size (Alegre et al., 2015). In contrast to jack mackerel, chub mackerel do not present a clear ontogenetic trend of consuming larger prey with increasing size; paradoxically, chub mackerel from all sizes foraged on small zooplankton (copepod) while small chub mackerel consume more fish than large chub mackerel (Alegre et al., 2015). Both jack mackerel and chub mackerel are considered opportunistic foragers, adapting their trophic behavior to prey accessibility (Alegre et al., 2015).

Saury or needlefish (*Scomberesox saurus scombroides*) is a pelagic fish that was abundant off Peru during the 1970s, when sardine dominated the HCS, reaching an estimated biomass of 1 million tonnes in 1978 (Jordán et al., 1978). In general, sauries spend most of their life in warm homogeneous surface layers of the open sea, far from shallow continental waters (Collette, 2004). In 1978 this species was mainly located between 30 to 60 miles off Peru (Jordán et al., 1978). When available, this species was also consumed by guano birds, although in low numbers (Jahncke and Goya, 1998).

2.2.4 Hake

Hake (*Merluccius gayi peruanus*) is a demersal species as an adult with semi pelagic behavior that is the target species of the main bottom trawl fishery of Peru (Guevara-Carrasco and Lleonart, 2008). Its area of distribution extends from 1ºN to 14ºS however most of the stock is located between 3ºS and 10ºS, and during El Niño the southern range extends to 18ºS (Chirichigno and Cornejo, 2001; Guevara-Carrasco and Lleonart, 2008). In recent years, juvenile hake were distributed mainly south of 5ºS while adults were mainly distributed north of 5ºS (Guevara-Carrasco and Lleonart, 2008). The main concentration of hake is between 100 to 200 meters depth but can be found from near the surface to 800 m (Guevara-Carrasco and Lleonart, 2008). Hake can tolerate hypoxic environments and thus it may be found at oxygen concentrations between 0.13 and 2.77ml.l^{-1}, however hake concentrations are not normally encountered below 0.25 ml.l^{-1} (Espino et al., 1995). Hake is an opportunistic predator that feed on several species; small hake (<25 cm) feeds on euphausiids whereas large hake (>25 cm) feeds on anchovy, euphausiids, pelagic shrimps, cephalopods and on other hakes (Tam et al., 2006).

2.2.5 Mesopelagic fishes

Mesopelagic fishes are small fishes from different families (e.g., Myctophidae and Photichthyidae), that live in the twilight zone of the ocean and perform diel vertical migration. During the day, they live at depth (200-1000 m) and have a reduced activity, while during the night they come to the upper 200 m or even to the surface to feed (Gjøsaeter and Kawaguchi, 1980; Kaartvedt et al., 2009). Myctophiids mainly predate on copepods, ostracods and euphausiids (Hopkins and Baird, 1985). Mesopelagic fishes likely dominate the world total fishes biomass (Irigoien et al., 2014), and *Cyclothone* sp. could be the most abundant vertebrate

on Earth (Nelson, 2006). Off Peru the mesopelagic community is dominated by the families Phosichthyidae (*Vinciguerria lucetia*), Myctophidae (*Diogenichthys laternatus* and *Lampanyctus idostigma*) and Bathylagidae (*Leuroglossus urotranus*; Cornejo and Koppelmann, 2006). The biomass of *Vinciguerria lucetia* during 2003 was estimated in 14 million tonnes (Castillo et al., 2009). Several species like *V. lucetia*, *D. laternatus* and *Lampanyctus sp*., among many others, have evolved physiological and morphological adaptations to live in oxygen-deficient waters, and perform diel vertical migration into the OMZ (Herring, 2001; Cornejo and Koppelmann, 2006), suggesting they may tolerate time periods of greater hypoxia.

2.3 Sedimentology of the Peruvian Margin

Sediment cores from the Peruvian margin show multiple discontinuities which makes efforts to reconstruct histories more difficult than sites like the Santa Barbara Basin or Saanich Inlet. Multiple sediment cores collected along the Peruvian margin, especially from 7 to 15ºS, show large hiatus of several thousands of years from the LGM to the Late Holocene (Skilbeck and Fink, 2006; Erdem et al., 2016). The discontinuities are more evident for the Holocene period, in particular for the Mid and Early Holocene (Erdem et al., 2016). The sediment structure of the sediment records is characterized by laminated sequences of several centimeters intercalated with homogeneous and slumped deposits (Brodie and Kemp, 1994; Salvatteci et al., 2014a). The homogeneous deposits may be produced by bioturbation or the addition of previously deposited material from upslope (Salvatteci et al., 2014a). Previous works have shown that marine sediments collected at ~14 and 15ºS show the most complete sediment sequence compared with sediment cores from the northern part of Peru (Doering et al., 2016; Erdem et al., 2016; Salvatteci et al., 2016). However, the records from the present study contain more laminated sequences compared with other cores taken from the same area (compare and contrast the sedimentological description provided for G-10 and G-14 in Salvatteci et al. (2016) and other sediment records in Erdem et al. (2016).

3. Material and Methods

3.1 Composite record and sub-sampling

The fish scale record presented in this work is based on a composite record from ~14 ºS, obtained from 1 box core (B05-14) that has high resolution records of the last several hundred

years and two long gravity cores, G-10 and G-14, covering the Holocene and the LGM-deglaciation respectively (Fig. 2). Dating of the box-core was done by ^{14}C on sedimentary organic matter and by ^{210}Pb means, while the two long gravity cores were dated by ^{14}C. The chronology models are fully described elsewhere (Salvatteci et al., 2014a; 2014b; 2016; 2018). B05-14 (93.6 cm length) recovered surface sediments and covers the time period from 1518 to 2004 AD (Salvatteci et al., 2014b). The gravity cores G-10 (5.22 m length) and G-14 (5.25 m length) do not recovered surface sediments and range from 0.45 to 10.3 kyr BP and 13.4 to 25.2 kyr BP respectively (Salvatteci et al., 2016). The description of the sedimentology and subsampling of core B05-14 is described in Salvatteci et al. (2014a, 2014b; 2018). The sedimentological description of G-10 and G-14 is available in Salvatteci et al. (2016) but is briefly described here. Core G-10 is characterized by sediment sequences containing finely laminated sediments interspersed with homogeneous sections and slumps (Fig. 2B). Core G-14 also shows the same type of structures as in G-10 but the thickness of the massive/slumped sequences is much lower (Fig. 2C).

Cores were subsampled after careful examination of the X-ray images of the sediment core to distinguish the laminated and homogeneous/slumped sections (Fig. 2). The laminated and banded sections of the core were subsampled and the slumped or homogenous sections were avoided. This methodology assures that the sediments used for our analyses were deposited from the water column and not from sediment re-deposition (Salvatteci et al., 2014a). Proxies developed from reworked sediment sequences could be misinterpreted as abrupt climate changes or anomalous climate events (Salvatteci et al., 2014a). Core B05-14 was subsampled following the stratigraphy resulting in sample thickness ranging from 0.15 to 0.84 cm; the average thickness was 0.45cm (Salvatteci et al., 2012). The fish scale record from core B05-14 was taken from Salvatteci et al. (2012, 2018). Cores G-10 and G-14 were subsampled every 1 cm for fish scales analyses. Fish scales analyses were mainly performed continuously in the laminated and banded sections, in some sections of G-10 only one out of two samples were analyzed (Fig. 2B). In core G-14 one sample out of five were analyzed (Fig. 2 C). The total number of samples analyzed in B05-14, G-10 and G-14 was 187, 202 and 91 respectively. Given the higher sedimentation rates and higher subsampling resolution of B05-14 compared with G10 and G-14,

in B05-14 contiguous samples were lumped to match the temporal resolution of G-10 (17.8 years) and G-14 (22.4 years) yielding a sample average of 19.6 years in B05-14.

The amount of sediment used is an important criterion that must be taken into account to obtain sufficient fish debris for reliable time series. In core B-14, where a fish scale preservation study was realized (Salvatteci et al., 2012), an average of 23.6 g of wet sediment was sieved which equals ~4.8 g of dry sediment. The quantity of fish debris in each of these samples was too low to perform statistical tests in some time intervals, some of which were characterized by strong fish scale degradation, and consequently five contiguous intervals were grouped to solve this issue (Salvatteci et al., 2012). Consequently, sampling intervals in core G-10 were larger, such that the average sample was 49.3 g of wet material, which yields ~17.2 dry sediment. In core G-14 sampling intervals consisted of an average of 39.2 g of wet material, which yields 18.8 g of dry sediment. Following the sediment subsampling, the samples were heated with a solution of hydrogen peroxide and sodium pyrophosphate for 10 minutes to disaggregate the organic matter and then were gently washed through a 355 μm sieve (Salvatteci et al., 2012). The remains retained were then stored in an alcohol solution.

3.2 Identification and quantification of fish debris

The fish debris retained in the 355 μm mesh size were quantified and identified with the help of a scale and vertebrae collection obtained from recently caught fishes (Fig. 3) and from the CICESE fish scale collection (Fig. 4). Fish scales were identified to species level for the following species: anchovy, sardine, jack mackerel, chub mackerel, hake, and saury. Fish scales from mesopelagic fishes (Fig. 4) were not identified to species level and were quantified as a whole group. The rest of the fish scales were quantified as unidentified. Vertebrae were identified to species only for anchovy and the rest of vertebrae were quantified as unidentified. Some vertebrae from *Vinciguerria lucetia* can be readily identified in the sediment record (bottom right in Fig. 3H) but other vertebra types (e.g. left vertebrae in Fig. 3H) cannot be easily distinguished of some vertebrae from other mesopelagic fishes. The most abundant vertebrae that were not identified were catalogued as types 1 to 13 but some types might belong to the same species (e.g. types 1 and 2). Pictures of vertebrae from several representative fishes of the HCS (e.g. sardine and jack mackerel) are available in Ostebase (http://osteobase.mnhn.fr), but very

few vertebrae in our composite record were conclusively identified as these species. In cores G-10 and G-14 the bones from the jaw were quantified in a separate category but in core B-14 were quantified as bones. Fish teeth were also quantified in all the cores as jaws. Spines were quantified as a whole spine if more than 50% of the original spine was present, the rest of spine fragments and segments were counted as spine fragments. Finally, the rest of the fish debris, as for example otoliths that were very rare, were quantified as bones. The quantification of fish debris (i.e. the distinction into complete, half scales and fragments) is described in Salvatteci et al. (2012).

The deposition of a part of a single fish can occur and results in a multitude of different debris from the same fish within a sampling interval (O'Connell and Tunnicliffe 2001; Field et al. 2009; Salvatteci et al., 2012). Thus, high fish debris abundance (more than the average + 3 standard deviations) of any fish debris component in our samples was treated as outliers (e.g. O'Connell and Tunnicliffe, 2001). The outliers were replaced by the mean plus 3 standard deviation. The occurrence of identified outliers is rare, the outlier replacement in cores G-10 and G-14 occurred in a maximum of 6 samples out of 293 samples in the case of anchovy scales, spines and other bones. Given the low abundance of sardine, jack mackerel, chub mackerel, hake and mesopelagic scales in the cores, the outlier treatment was not applied in these cases even if some samples exceeded the mean plus 3 standard deviations.

Since the concentration of fish debris (# of fish debris$\times g^{-1}$) can be diluted (increased) by low (high) mass accumulation rates, concentrations of fish scales and bones were converted to fluxes (# debris$\times cm^{-2}\times y^{-1}$). The fluxes of each fish debris component were calculated by multiplying the fish debris abundance (# of fish debris$\times g^{-1}$) by the mass accumulation rate (W, $g\times cm^{-2}\times y^{-1}$), in turn W is calculated multiplying the Dry Bulk Density (DBD, $g\times cm^{-3}$) by the sedimentation rate ($cm\times y^{-1}$). The mass accumulation rates are taken from Salvatteci et al. (2016). Since the mass accumulation rate is in turn dependent on the presence of hiatus, or slumps within the sedimentary column, estimated fluxes are subject to uncertainty and/or variability in sedimentation rates. The fish scale data is also presented as concentrations (#of fish debris per g^{-1}) in the supplementary material (Figs. S1 and S2). The major downcore patterns are similar regardless of units. However the very high fluxes of debris observed for the last 150 years are not

observed in the concentrations (e.g. sedimentation rates are also higher). Finally, given that the calculated fluxes were relatively small, the values were multiplied by 1000 to be consistent with other published reports of scale fluxes.

3.3 Fish debris preservation

In order to quantify the effect of degradation, we estimated three preservation indices, and an average of all the indices, based on previous studies in the same area (Salvatteci et al., 2012). The first degradation index, the "integrity index" of fish scales, is an estimate of fish debris wholeness relative to fragmentation. This index is based on scales from all species to obtain an index; ideally the index would be species specific (Salvatteci et al., 2012) but there were insufficient scales counted for a species-specific index. The second index is the "bio-degradation" over fish vertebrae, which estimate the surface of the vertebrae that is not affected by bio-erosion. Finally, the last index used is the ratio of all scales to vertebrae, based on the observation that fish scales are thinner, contain more organic matter than the vertebrae, and consequently are more susceptible to degradation. Given that these indices have different units, they were standardized and then the three indices were averaged to create a compound preservation index. Higher (lower) values of these indices indicate better preservation of the fish remains. A detailed explanation of the advantages and limits of these and others indices are explained in Salvatteci et al. (2012).

Electron microscopy images were also taken to gain insight about the process of fish debris degradation by comparing fish scales and vertebrae extracted from a modern anchovy with poorly preserved fish debris from the sediment record. SEM observations were performed at IRD-Bondy (France) on uncoated samples using a Zeiss Evo® LS15 microscope (Carl Zeiss Ltd, UK) in variable pressure mode (VP) at an accelerating voltage of 15 kV, with a chamber pressure of 70 Pa and a 100 µm VP aperture.

3.4 Proxies for export production and oxygenation

The fish debris records and the preservation indices were compared to proxies of environmental change to understand the mechanism that control fish scale preservation and fish population variability off Peru. In order to identify the effects of the oxygenation changes in the

fish scales preservation, the different fish scale preservation indices were compared to proxies of oxygenation taken from the same composite record (Salvatteci et al., 2016). The proxies used for this purpose are: 1) Mo/Re ratios which indicate if the sediment-water interface during the time of deposition was anoxic or sub-oxic (Crusius et al., 1996), and 2) $\delta^{15}N$ values measured on bulk sedimentary organic matter which indicate the extent of water column denitrification in oxygen-deficient waters and thus sub-surface oxygenation (Ganeshram et al., 2000). To establish the relationship between OMZ intensity and fish abundance the $\delta^{15}N$ values were used because this proxy better reflects changes in water column oxygenation.

In order to establish the relationship between export production and fish abundances, we used three proxies for export production: Total Organic Carbon (TOC), Nickel Enrichment Factor (Ni EF) and calcium carbonate. The TOC reflects the amount of organic carbon present in the sediment and can be used to infer past export production. Ni is delivered to the sediment mainly in association with organic matter and thus is an indicator of the organic sinking flux (Böning et al., 2105). In contrast to organic matter that can be remineralized by bacterial activity, Ni may be retained within the sediments and thus could represent the original presence of organic matter even if it is lost after deposition (Tribovillard et al., 2006). Calcium carbonate in marine sediments is basically composed of skeletal remains of calcite secreting organisms (e.g. foraminifera), but detrital calcium (i.e. gypsum) can also be delivered to the ocean by winds and rivers.

In G-14 Mo, Re, Ni, $CaCO_3$, TOC and $\delta^{15}N$ were obtained in the same samples as the fish debris records (91 samples). In G-10 Mo, Re, Ni were obtained in 200 samples but $CaCO_3$ was analyzed in 171 samples. The subsampling for $\delta^{15}N$ and TOC in G-10 was done every 2 cm yielding in total 130 samples. In B05-14, Mo, Re, Ni, $CaCO_3$, TOC and $\delta^{15}N$ data were produced at high resolution (Salvatteci et al., 2014b; 2018) but the data were lumped to match the temporal resolution of cores G-10 and G-14. Mo, Re, Ni and Ca concentrations were obtained by ICP-MS (Ultramass Varian) after hot-plate acid digestion in Polytetrafluoroethylene vessels. Mo, Re, and Ni data was taken from Salvatteci et al. (2016) while the Ca data were not previously published. The calcium carbonate ($CaCO_3$) content was estimated by multiplying the Ca concentration (%) by 2.5 according to the atomic weights of the elements. The TOC values were obtained using

Rock-Eval 6 and the data was taken from Salvatteci et al. (2016). $\delta^{15}N$ values were measured in untreated sediment samples (i.e. no acidification methods were used) on a continuous-flow gas-ratio mass spectrometer (Finnigan Delta PlusXL) coupled to an elemental analyzer (Costech) and the data was taken from Salvatteci et al. (2016).

3.5 Statistical analyses

Given that counts of fish remains have a large number of zeros, a non-Gaussian distribution of the data results, which limits the use of most parametric methods. Thus, Spearman correlation coefficients (r_s) were calculated to establish the relationships between different types of fish debris as well as between selected fish debris fluxes and proxies of environmental conditions. The probability level was corrected for multiple comparisons by dividing the probability level α ($p<0.05$) by the number of tests performed (Glantz, 2002). In order to test for differences of fish debris fluxes between the different time-periods, a Kruskal-Wallis test was applied. In addition, to better explore non-linear relationships, we used Generalized additive models (GAMs) applying the Tweedie versatile family distribution (Dunn and Smyth, 2005), which are commonly used to represent distributions that have a non-zero probability for the zero value. Still the number of zeros was still too high in some cases (e.g. sardine). Thus, we could only test for the relationships of anchovy vertebrae, anchovy scale, oceanic species scales, hake scales and mesopelagic fish scales versus Ni EF and $\delta^{15}N$.

Finally, in order to detect structure in the relationships between variables that might lead to infer processes, a Principal Component Analysis (PCA) was performed using a sub-set of the variables. The PCA analysis was performed to: (i) examine if the fluxes of anchovy and other species vertebrae are more associated with oxygenation or productivity, and (ii) examine if the degradation indices are more closely associated with changes in oxygenation in the water column or in the sediment. The statistical analyses were performed using STATISTICA 13 and R.

4. Results

4.1 Fish debris composition

In total nearly 120,000 pieces of fish debris were classified and counted in the composite record and fish scales were the most abundant type of fish debris (Table 1). Fish scale fragments

were about 5 times more abundant than whole fish scales. Spines and spine fragments were more abundant than other bones, and each of these were 3 to 4 times more abundant than vertebrae (Table 1). Fish vertebrae were not as abundant as spines or other bones but were also found consistently throughout the core. Most vertebrae were very small and thin, and examples are displayed in Figure 5. The fluxes of each type of vertebrae is available in the supplementary material (Fig. S3). Jaws containing teeth were also part of the fish debris but in lower abundance compared with the other fish debris types. Otoliths were rare and were only found in very few samples, perhaps due to aragonite dissolution in the sediments.

The composition of fish scales by species (Table 2) reveal a clear predominance of anchovy scales (~90% all scales). Fish scales from mesopelagic fishes (2.9%) and from hake (2.7%) were the next most common. The oceanic species comprised 2.8% of all the fish scales counts and were primarily composed of sardine and jack mackerel, with smaller contributions from chub mackerel and saury. The unidentified scales represented 1.9% of all fish scales, but since most anchovy scales were readily identifiable, these scales made up 22% of scales other than anchovy.

4.2 Fish debris record

The relationships between the different types of fish debris reflect the modes of loss, transport and preservation of the different types of fish debris (Table 3; Fig. 6). The anchovy scale record has a high significant correlation with fish scale fragments (r_s=0.89, n=317, p<0.001) suggesting that most of the fragments belonged to anchovy, consistent with the appearance of the fragments as being from anchovy. In contrast, the correlations of the different types of bones (i.e. other bones, jaws, spines and spine fragments) were only slightly higher with anchovy vertebrae than with other vertebrae (though significant for each type of vertebrae) suggesting that the majority of the bones belong to anchovy, but other species also contribute noticeably (Table 3). The sum of all fish scales (Fig. 6A) was highly correlated with the sum of all bones (r_s=0.62, n= 317, p<0.001; Fig. 6D), while anchovy scales (Fig. 6B) and anchovy vertebrae (Fig. 6H) were also positively correlated (r_s=0.42, n=317, p<0.001). The correlations calculated with concentrations instead of fluxes (Table S1) also show the same pattern of association between variables.

The lack of a better correlation between fish scales with bones can be explained by temporal differences in the abundance of the different types of fish debris along the record. For example, during the Termination 1 a relative increase of fish scales compared with the fluxes of all bones was observed for both the sum of all species and anchovy (Fig. 6A, B and D). Moreover, the correlations among the different types of the fish bones (i.e. jaws, spines, spine fragments and vertebrae) were all significant and in general higher than the correlations of these skeletal debris with the fish scale fluxes (Table 3). This observation suggests that fish bones and fish scales have different modes of loss and transport to the sediment and that fish scales and bones preserve differently in the sediments. However, the correlation of anchovy scales to spines was higher than the correlation of anchovy scales with any other fish bone type. This implies that spines, which are the thinnest bone debris and thus more prone to degradation, and anchovy scales may have a similar response to the degradation processes and/or that spines more frequently come from anchovy.

The different fish debris types are shown as time series in Figure 6 as well as averages of major climate periods in Figure 7 to better illustrate the temporal changes in the fluxes of the different fish debris types. The concentrations of the different fish debris types expressed as concentrations are shown in Figures S1 and S2. Considerable variability in fluxes occurred over the last 25 kyr BP, for example low fluxes of most of the fish debris types during the glacial period and high fluxes during the Holocene (Figs. 6 and 7). However, some important temporal differences between scales and bones were observed. For example, higher fluxes of anchovy scales (Fig. 7B) occurred during the Termination 1 compared with the LGM, while no large differences in anchovy vertebrae fluxes (Fig. 7L) were observed between these two periods. A Kruskal-Wallis test shows that the fluxes of all fish scales, anchovy scales, and scale fragments were significantly lower during the glacial periods than any other period (Table S2, S3 and S8). While the fluxes of anchovy vertebrae during the glacial times were also significantly lower compared with the Holocene, there were no significant differences in the fluxes between the glacial periods and the Termination 1 (Table S9).

While the Holocene had higher fluxes of various types of fish debris compared with the glacial and Termination 1 periods, there were important differences between the fluxes of fish scales and bones (Figs. 6 and 7) between different time periods, which could reflect differences in preservation. During the Early Holocene, the fluxes of fish scales from all species and of anchovy were significantly lower (Table S2 and S3) than during the Termination 1 period. In contrast, anchovy vertebrae fluxes were significantly higher during the Early Holocene compared with Termination 1 (Table S9). A gradual increase in the fluxes of all scales, anchovy scales and hake scales is observed from the Early Holocene to the Late Holocene (Figs. 7A, B and D). However, no clear trend is observed in the fluxes of all bones, spines, spine fragments, other bones, vertebrae and jaws from the Early to the Late Holocene (Fig. 7H-N). While the fluxes of anchovy and hake scales were significantly higher during the Late Holocene compared with the Early Holocene (Table S3 and S5), no differences were observed in any type of fish bone fluxes between the Early, Mid or Late Holocene periods (Fig. 7; Tables S9-S13). Finally, the fish scale fluxes from all species, anchovy and mesopelagic fishes were significantly higher, by at least one order of magnitude, during the Current Warm Period (CWP) compared with any other period (Tables S2, S3, and S6). The fluxes of the different types of fish bones were not statistically different during the CWP when compared with any Holocene period (Fig. 7; Tables S9-13), except for the fluxes of fish vertebrae from other species that were significant higher during the CWP compared with any of the other time period (Tables S10).

4.3 Fish scale preservation and SEM observations

The preservation indices, the scales and vertebrae fluxes of anchovy and proxies for environmental variability are all shown in Figure 8 and support the idea that the greater number of bones than fish scales in periods characterized by enhanced oxygenation could be due to fish scale degradation. Overall the three preservation indices show similar temporal patterns but were not highly correlated with one another (Table 3). Given that each of the three preservation indices can be affected by factors other than degradation, the compound preservation index is likely the best indicator of fish scale preservation for the record (Fig. 8K; Salvatteci et al. 2012). The compound index showed low values (indicating poor preservation) from the glacial period to ~18 kyr BP and high values during part of the deglaciation (i.e. Termination 1), but with greater degradation from ~15 to 13.5 kyr BP. The Early and mid-Holocene were characterized by

relatively low values (poor preservation) like those of the glacial period, while the last 3 kyr showed higher values compared with the rest of the Holocene but lower values compared with most of the Termination 1 period.

While the major downcore patterns were shared between each preservation index, only some of these temporal changes were associated with significant differences in preservation indices between periods (Figs. 7P-R, and 8H-J). In the case of the integrity index, higher degradation was only detected during the Early Holocene (Table S14). The index of bio-erosion was higher (indicating less area covered by bio-erosion and thus good preservation) during the CWP and the Termination 1, with no statistical difference between these periods (Table S15). During the CWP and Termination 1 periods, the bio-erosion index indicates better preservation compared with the Holocene and glacial periods (Table S15). The ratio of scale to vertebrae was high during the CWP and the Termination 1 period (no statistical difference between these periods) and very low during the Early Holocene and the glacial period (Table S16). The compound preservation index was also high during the CWP and the Termination 1 period (not statistical difference between these periods) and significant lower during the glacial period and during the Early Holocene compared with both the Termination 1 and the CWP (Table S17).

SEM observations of fish scales reveal some of the processes of degradation of fish scales by biota producing bio-erosion traces (Fig. 9). The two well-defined portions of the anchovy scale, the hard upper well-mineralized portion and the multiple layers of fibrous collagen, are readily identifiable in anchovy scales from a recently caught specimen (Fig. 9A-D). The hard well mineralized portion is characterized by the growth lines over the fish scale surface and is very thin in comparison with the middle portion composed of collagen layers (Fig. 9B and C). The organic-rich collagen layers arranged in a lamellar fashion represent the thickest part of the fish scale (Fig. 9B). An anchovy scale that has signs of bio-erosion all over the scale (Fig. 9E) by conventional microscopy showed no apparent signs of visible bio-erosion over the surface under SEM (Fig. 9F). However, a detailed observation reveals the presence of small holes in the upper-well mineralized section of the scale (black arrows in Fig. 9G and H). These observations suggest that bio-eroders penetrated the external layer to access the protein-rich internal layers. A vertical section of the same scale shows several burrows and channels dug by bio-eroders within

the collagen layers (Fig. 9I- K). An anchovy scale that shows parts of the upper hard layer detached from the scale (Fig. 9L), has multiple needle-type structures. Another type of degraded fish scale described by Salvatteci et al. (2012) was the thin and rolled-up scales with little structural support (Fig. 9M). SEM images show evidence of bio-erosion all over this type of scale and a presumably lack of the collagen layers that caused the reduced thickness in this poorly preserved fish scale (Fig. 9N- P).

Anchovy vertebrae were also partially consumed by biota that leave bio-erosion traces. However, the vertebra maintained its rigidity even if multiple bio-erosion traces were present in the vertebra (Fig. 10). The images of an anchovy vertebra from a recently caught anchovy (Fig. 10A-C) show the cavities in the bone structure (Fig. 10B) where the dorsal spines were attached (two oval shaped structures in Fig. 10A). A vertical section of the same vertebra (Fig. 10C) shows lower quantity of cavities in the internal area. The SEM images of a half of an anchovy vertebra with bio-erosion traces all over (Fig. 10D-F) show multiple burrows and channels inside the vertebrae (compare and contrast Fig.10C and 10F). This anchovy vertebra was characterized by extensive evidence of bio-erosion in comparison with the other vertebrae found in the sediment cores. Holes were observed only in the cracked section of the vertebrae, not in the external layer of the vertebrae (Fig. 10E-F).

Another type of fish debris alteration can be observed in some vertebrae from the glacial period (Fig. 10G-I). SEM images of one vertebra from the LGM show the presence of unidentified mineral phases forming over its surface. Additionally, the surface of this vertebra presented thin layers over the vertebrae, as observed in the bottom-left section of Fig. 10H, which could be easily detached with a pincer. The burrows (Fig. 10E-F) and the mineral phases that were formed over the vertebrae (Fig. 10H-I) did not cause an evident increase in the fragility of the vertebra even during the LGM which is associated with the lowest fluxes of anchovy scales, poor preservation and a weak OMZ (Fig. 8). This observation suggests that the fish vertebrae are much less likely to dissolve and changes in their abundances can be used as a rough proxy for fish population variability during periods of poor fish scales preservation.

The relationship between the compound preservation index with $\delta^{15}N$ as a proxy for denitrification and hence water column oxygen was high and significant, while the relationship between the preservation index and sediment redox conditions (Mo/Re) was not as good but still significant (Table 3). Both the $\delta^{15}N$ and the Mo/Re records presented a similar pattern during the glacial periods and the Holocene, with lower values during the glacial period, the mid-Holocene and parts of the Late Holocene indicating a weaker OMZ and higher values during most of the Holocene indicating a stronger OMZ (Fig. 8A-B). However, at the start of the Termination 1 the Mo/Re increased slightly and then decreased, which is in contrast with the sustained high values of $\delta^{15}N$ during this period (Fig. 8A-B). The preservation indices also show high values during the Termination 1, with a similar pattern as the $\delta^{15}N$ record (Fig. 8A, H-K). The individual preservation indices also have stronger relationships with $\delta^{15}N$ than with Mo/Re (Table 3), though the relationships are not as strong, which confirms that the compound index is a better representation of preservation.

4.4 Fish species composition and relationships between species

The assemblage of fish scales during the last 25 kyr BP was largely dominated by anchovy but other species contributed noticeably in some periods (Fig. 11). During the glacial period, fish scale fluxes from all species were low, but the scales of oceanic species were very scarce (Fig. 11B-E). The end of the LGM was characterized by the presence of jack mackerel, hake and mesopelagic fishes (Fig. 11C, F-G), then 2 kyr later, fluxes of anchovy scales increased (Fig. 11A). The rest of the Termination 1 period was marked by high fluxes of anchovy and mesopelagic fish scales, relatively high fluxes of saury and the absence of sardine and chub mackerel scales.

During the Holocene high fluxes of anchovy and mesopelagic fishes were observed, as well as high fluxes of oceanic species compared with the glacial periods and the Termination 1 (Fig. 11). The Early Holocene was characterized by relatively high fluxes of fish scales from oceanic species, anchovy and mesopelagic fishes, but low abundance of hake. The ratio of scales from oceanic species to anchovy was highest during the Early Holocene presenting then a slight decreasing trend towards the CWP (Fig. 7O). Within the sediments present of the Mid Holocene, relatively high fluxes of anchovy and low fluxes of oceanic species, hake, mesopelagic fishes

and unidentified fish scales were observed (Fig. 11). The Late Holocene was characterized by high anchovy scale fluxes and an increase in hake scale fluxes (Fig. 11A, F). Finally, during the CWP the flux of anchovy scales were one order of magnitude higher in comparison to the rest of the record, and also the fluxes of oceanic species, hake, and mesopelagic fish scale fluxes are relatively high (Fig. 11). The fluxes of fish scales from unidentified species were higher during the CWP but also during the start of the Termination 1 period (Fig. 11H). Nevertheless, they still represented a low percentage of the fish scale assemblage.

Relationships between time series of fish scales from different species could help to understand the temporal changes in the marine ecosystem off Peru (Table 4). Given the poor preservation of fish scales during some intervals and that fish scales from the different species may have different responses to degradation due to their differences in size and thickness, we focus on the well-preserved intervals of our composite record (values higher than 0 in the composite record, Fig. 11I) to gain insight on the relationship between species and between the proxies of environmental variability. Contrary to the negative relationship that characterize the anchovy and sardine landings in the HCS during the last 60 years, anchovy and sardine scales fluxes showed a weak positive but not significant correlation (Table 4; r_s=0.20, n=135, p>0.004). Fluxes of anchovy scales also showed a poor correlation with the other species (Table 4). Among the oceanic species, jack mackerel and chub mackerel were highly correlated (r_s=0.34, n=135, p<0.004), which was expected since these species share some similarities in habitat, physiology and behavior. The scale fluxes of mesopelagic fishes was also highly correlated with jack mackerel (r_s=0.38, n=135, p<0.004). The correlation of jack mackerel with mesopelagic fishes were higher than the correlation of anchovy with mesopelagic fishes which was also expected given that anchovy inhabits the coastal area while jack mackerel and mesopelagic fishes prefer the offshore region. These relationships between species were similar when the fish concentrations (Table S18) were used instead of the fluxes meaning that the relationships between species is not driven by temporal changes in mass accumulation rates.

Relationships between fish scales and fish vertebrae from different species could give an indication to which species the unidentified vertebrae might belong. The fluxes of scales of mesopelagic fishes and other vertebrae showed similar downcore patterns (Fig. 6I and 11G) and

were highly correlated (r_s=0.51, n=135, p<0.001), suggesting that a great part of the unidentified vertebrae shown in Figure 5 belong to these species. Anchovy scales were also highly correlated with other vertebrae (r_s=0.44, n=135, p<0.001) suggesting that some of the unidentified vertebrae, like the type 4 and 5 vertebrae, could belong to juvenile anchovies.

4.5 Fish debris records and proxies for environmental variability

Relationships between the different types of fish scales and $\delta^{15}N$, the proxy for water column denitrification, could indicate the role of sub-surface oxygenation driving changes in fish populations. To understand the role of oxygenation on fish population variability we only focused on the well-preserved intervals (n=112; Fig. 11I). A strong and positive correlation was only observed for anchovy scales and $\delta^{15}N$ (r_s=0.38, n=112, p<0.001) while the correlations of the other fish scale fluxes with $\delta^{15}N$ were poor (Table 4). Additionally, the GAM results indicate a positive and strong relationship between anchovy scales and $\delta^{15}N$ (Fig. 12B). In contrast, there is a positive relationship between anchovy vertebrae and $\delta^{15}N$ only for the low $\delta^{15}N$ values, at higher $\delta^{15}N$ values there is no relationship (Fig. 12A). This suggests that a strong OMZ is favorable for anchovy. The results from the GAMs showed no clear relationship between $\delta^{15}N$ and hake the oceanic species or the mesopelagic fishes (Fig. 12C-E) as also observed in the poor correlation of these fishes with $\delta^{15}N$ (Table 4).

Considerable variability in productivity, as inferred by Ni EF, TOC, and $CaCO_3$, occurred over the last 25 kyr BP, for example low productivity during the glacial period and high productivity during parts of the Holocene (Fig. 8C, D and E). However, some important temporal differences, specially between the $CaCO_3$ fluxes and the Ni EF record, were observed. The correlations (Table 3) of the TOC fluxes with Ni EF and CaCO3 are strong and positive (r_s=0.40, n=245, p<0.001; r_s=0.30, n=215, p<0.001 respectively), while there is no correlation of Ni EF with $CaCO_3$ (r_s=-0.13, n=284, p<0.001). Part of the strong correlation between TOC and $CaCO_3$ fluxes might be due to transformation of the concentrations into fluxes given that there is no correlation in the concentrations of TOC and $CaCO_3$ (Table S1); in contrast to the correlation of TOC and Ni EF which is strong in both fluxes and concentrations (Table 3 and Table S1). The three productivity proxies show low values during the glacial period and both Ni EF and TOC

show a slight increase during the Termination 1 period compared to the glacial period (Fig. 8C-E). However, the $CaCO_3$ record shows a strong increase during the Termination 1 period compared to the glacial period (Fig. 8 E). During the Holocene the Ni EF record shows low values during the Early and mid-Holocene and high values during the Late Holocene though with strong centennial-scale variability (Fig. 8C). The record of TOC fluxes also shows low values during the Early Holocene and from 2 to 0.5 kyr BP, with high values from ~5 to 2 kyr BP, and the highest values during the CWP (Fig. 8D). During the Holocene the $CaCO_3$ record shows low values with some time intervals characterized by high $CaCO_3$ fluxes, as for example at ~9.5 kyr BP and during the CWP (Fig. 8E). Given that the Ni EF better represent the original presence of organic matter, is not affected by changes in sedimentation rates (as is the case of the TOC fluxes) and has a higher temporal resolution (compared with the TOC and $CaCO_3$ data) henceforth we use the Ni EF as a proxy for export production.

The correlations and the GAM results between the different types of fish debris with export production reveal the role of marine productivity driving temporal fluctuations in the fish debris records (Table 4; Fig. 12). To understand the role of export production on fish population variability we only focused on the well-preserved intervals (n=135, Fig. 11I). The export production record (Ni EF) presented relatively high and significant correlations with the scale fluxes of anchovy (r_s=0.27, n=135, p<0.001), sardine (r_s=0.45, n=135, p<0.001) and chub mackerel (r_s=0.31, n=135, p<0.001), while the relationships of hake and mesopelagic fishes with export production were positive but not significant (Table 4; Figs. 12I and J). Moreover, Ni EF and anchovy vertebrae also showed a strong and positive correlation (r_s=0.36, n=135, p<0.001). Once more, the correlations of fish scale concentrations with Ni EF are similar as the correlations of fish scale fluxes with Ni EF (Table S18), suggesting a strong relationship of productivity with some species. The strong relationship between productivity and anchovy is also evidenced in the GAMs results (Fig. 12F and G). The GAM for the oceanic species also shows a positive relationship with productivity (Fig. 12H). However, time intervals with high Ni EF values are often associated with very high $\delta^{15}N$ values and low oceanic species abundance (Fig. 8A and C, Fig. 11B-E), thus sub-surface oxygenation might be limiting an increase in oceanic species abundances when food is available.

Based on 19 selected variables over the length of whole data set (n=317), the PCA results indicate that most variance of the data set (60.6%) was encompassed by the first three principal components (Fig. 13). The temporal records of these principal components are shown in Figure 14 alongside five records that best reflect the temporal variability of each PC (see also supplementary Text 1). PC1 is interpreted as the fish production signal excluding the oceanic fishes and has a similar pattern as the fluxes of all fish scales excluding the oceanic species (Fig. 14B). PC1 has the highest loadings for all fish scales, scale fragments, anchovy scales, mesopelagic scales, the bone remains and TOC.

PC2 is interpreted as a signal of preservation. PC2 has the highest positive loadings for anchovy vertebrae and other bones, and the highest negative loadings for the three degradation indices, $\delta^{15}N$ and Mo/Re. This means that when anchovy vertebrae and other bones are relatively abundant compared with anchovy scales, there is not good preservation of scales due to higher oxygen concentrations.

PC3 is interpreted as the fish production of oceanic species (Fig. 14F) and its impact on the fluxes of fish vertebrae to the sediments given that it has the highest negative loading for the fish scales of oceanic species and the highest positive loading for the ratio of scales to vertebrae. An increase in predation of the oceanic species on anchovy could produce an increase in the flux to the sediments of bones and vertebrae relative to fish scales given that fish scales are easier to be digested than bones (O'Connell and Tunnicliffe, 2001). Alternatively, more oceanic species could result in more of their vertebrae making it to the sediment. The PCA analysis was also performed using the concentrations instead of the debris fluxes (Figs. S4 and S5), but the results are very similar, indicating that the conversion of the fish concentrations to fluxes did not drive the association among variables.

5. Discussion

A stacked record of fish debris covering the last 25 kyr BP, collected in one of the most productive marine areas off Peru, was compared with proxies of environmental conditions to test for effects of temporal changes in the intensity of the OMZ and productivity on fish population abundance on multidecadal to millennial timescales. The range of glacial to interglacial

conditions provides a wide range of oxygen and productivity combinations that reflect several end member oceanographic states of this region of the Humboldt Current (but not including the dramatic interannual El Niño/ La Niña changes).

Taken together, the evidence from scales, skeletal debris, preservation indices, and oxygen indices suggests that fish scales deposited in laminated sediments should only be used to reconstruct past fish populations during periods associated with low oxygen contents in the water column and in the sediments. For periods associated with greater oxygenation, and thus poor preservation of fish scales, vertebrae may be a better indicator of fish abundance.

Our records show that anchovy was the most abundant pelagic fish in the NHCS during the last 25 kyr, which is consistent with low resolution fish scale records from the Central Peruvian Margin (De Vries and Pearcy, 1982). During the last 25 kyr, anchovy abundance reached a maximum during the CWP i.e., when the industrial fisheries arose. Productivity seems to be a main driving factor of anchovy, sardine and other species fluctuations (Table 4). On the other hand, while oxygen is important to fish scale preservation in the sediments, the relationship between changes in oxygen with population variability of most species is less clear. However, anchovy seem to flourish during periods characterized by a strong (not the strongest) OMZ like the CWP. It is, however, important to account for the step size of our data when interpreting our results and the potential mechanisms. Indeed our dataset ranges over 25 kyr but the sample step size varies between 6 and 50 years with an average of ~20.4 years. These time steps probably capture the long-term averages but do not resolve sub decadal to decadal scale changes associated for example with anchovy and sardine fluctuations. In the following sections we discuss the importance for an accurate fish debris identification, the mechanisms driving fish scale preservation, and finally the changes in fish population variability during the last 25 kyr BP.

5.1 The utility of vertebrae and fish scale preservation

Difficulties with vertebrae identification result in the very high number of unidentified vertebrae that probably belong to mesopelagic species and/or to juveniles from other species. Vertebrae morphology vary within a species along the vertebrae column (Fig. 3G; Rose, 2013) as

do fish scales (Fig. 3A-C). While the identification of fish scales and vertebrae from the most commercially important fishes (Fig. 3) could be readily done, the identification of fish scales and vertebrae from other abundant fishes like the mesopelagic fishes was a challenge. The work by Patterson et al. (2011) is perhaps the most detailed fish scale Atlas for the North Pacific, and Osteobase (http://osteobase.mnhn.fr/) contains several vertebra types of multiple fish species. However, none of these works contain information about fish scales and vertebrae from mesopelagic fishes or fish of different ages. It is clear that to better understand past changes in fish communities, other than anchovy, sardine, jack mackerel, chub mackerel and hake, a comprehensive atlas of fish vertebrae is needed.

While previous studies (De Vries and Pearcy, 1982; O'Connell and Tunnicliffe, 2001; Salvatteci et al., 2012), have shown strong changes in fish scale preservation in marine sediment records, changes in oxygenation during fish debris burial and not time after burial, seem to be the main driver of fish scales degradation in the sediment record. This principle is clearly evident since poor fish scale preservation occurs during periods associated with a weak OMZ, and enhanced water column oxygenation, like the LGM and the LIA (Fig. 8K; Salvatteci et al., 2012). Likewise, fish scales from parts of the Termination 1 period, that encompassed a strong OMZ, are similarly preserved compared with fish scales from the last 150 years (Fig. 8K).

The present study builds upon a previous study (Salvatteci et al., 2012) in terms of identifying preservation with multiple indices and using vertebrae as an indicator of population variability when preservation of scales is poor. For longer sediment records containing periods associated with strong changes in oxygenation, vertebrae could be used as indicators of relative changes in fish abundance. However, there are several factors that need to be considered while using vertebrae data. First, fish scales reach the water-sediment interface primarily from scale shedding (Shackleton, 1988; Field et al., 2009), while the majority of bones and vertebrae reach the sediment by passing through the guts of predators (O'Connell and Tunnicliffe, 2001; Field et al., 2009; Salvatteci et al., 2012). Thus, although the fluxes of fish scales and vertebrae to the sediments should be somewhat dependent on population size, different modes of loss and transport of vertebrae could cause deposition patterns to differ from those of scales (Salvatteci et al., 2012). For example, an increase in the abundance of jack mackerel during the Early

Holocene in our records might be partly responsible for the relatively high abundance of anchovy vertebrae compared with the anchovy scales (Fig. 7B and L). Second, the vertebrae are scarcer in comparison with fish scales and other type of fish debris (Table 1) and thus large quantities of sediment must be analyzed to obtain a representative sample. Third, the difficulties associated with fish bones identification makes this procedure a challenging task. In our composite record the vast majority of the large vertebrae corresponded to anchovy and the small vertebrae to unidentified species that very likely belong to mesopelagic fishes or juvenile individuals (Fig. 5). Specifically, the lack of a defined waist in types 4 and 6 (Fig. 5) and the lack of well-developed neural spines suggest that these vertebrae could belong to juvenile fishes (Rose, 2013). The presence of vertebrae identified to be from jack mackerel, chub mackerel, hake or sardine was rare.

Both the observations of scales and vertebrae and the different relationships between the preservation indices with $\delta^{15}N$ and Mo/Re (Table 3), suggest that there are multiple ways in which scale degradation occurs and that oxygenation in the water column or in the sediments might also affect the indices in different ways. The strong correlation between the bio-erosion index with $\delta^{15}N$ suggests that a more oxygenated water column may allow bio-eroders to colonize scales in the water column or shortly after arrival to the sediments. Additionally, the correlation of the ratio of scales to vertebrae with water column denitrification was higher than with sediment redox conditions. One possible interpretation is that periods with a strong OMZ limits the inshore incursion of predators (Bertrand et al., 2016), reducing predation and thus the fluxes of fish vertebrae (and other bones) to the sediment floor. Finally, the integrity index is sensitive to the number of scales counted and thus may not be powerful enough to detect the poor preservation of fish scales that occur for example during the glacial period that was observed during the process of fish debris identification. Perhaps an additional preservation index based on the fish scale coloration and/or texture can be useful given that the few fish scales from the glacial periods showed noteworthy changes in color and texture. These fish scales were yellowish and crumbled apart very easy.

Fish scale degradation is driven by the premise that micro-organisms will nourish themselves on the fibrous and organic-rich collagen layers (Fig. 9). Although the mineralized

external layer is avoided by these organisms, they need to perforate this thick layer in order to reach the collagen fibers. Very few holes were found in the external layer while the internal collagen layers were full of burrows and channels in the fish scales characterized by strong degradation (Fig. 9). The bio-eroders could not be identified and could belong to any of the following taxa: cyanobacteria, chlorophytes, fungi and other micro-chemotrophs (Wisshak et al., 2011), and not only fungi as proposed by Salvatteci et al. (2012). One implication of the strong degradation of fish scales in Peruvian sediments is that isotopic analyses on fish scales (Struck et al., 2002; Hutchinson and Trueman, 2006) may be affected by the effect of bio-eroders on fish collagen, and that only pristine scales should be used for this type of analyses.

5.2 Fish population variability

Based on our 25 kyr record, productivity appears as the main factor controlling small pelagic fish abundance (Table 4). Then, sub-surface oxygenation seems to play a role regulating the abundance and distribution of pelagic fishes in the HCS in a species-dependent way. Indeed, the abundance of most of the species increased with productivity while anchovy seems to flourish in periods associated with a strong OMZ and high productivity, but the oceanic species need more oxygen to thrive (Figs. 8 and 14). Taking into consideration fish scales preservation in the sediments and the sampling volume, the largest resolved changes in inferred fish abundance in our records occurred over centennial to millennial timescales (Figs. 8, 11 and 14).

5.2.1 Glacial Periods

The low inferred abundance of all fish species during the glacial periods is likely due to lower productivity (Figs. 11 and 14). Although poorer preservation of scales during the glacial could affect the reconstruction of total fish abundance, particularly of the rarer species, the lower number of vertebrae reiterate that abundances of most taxa were lower. The climatic and oceanographic conditions off Peru during the cold glacial periods were not favorable for primary productivity and for pelagic fishes in general. While SSTs during the LGM may have been lower in the ETP (Feldberg and Mix, 2003; Koutavas and Joanides, 2012) and also in the HCS (Rein et al., 2005; Salvatteci et al., 2019), the cooling could be caused by changes in the strength and/or temperature of advection off the eastern boundary and not primarily by upwelling of cold waters (Feldberg and Mix, 2003; Salvatteci et al., 2019). Moreover the ITCZ experienced a southward

shift in its position, implying a decrease in equatorial upwelling (Koutavas and Lynch-Stieglitz, 2004). The few sediment records collected in the Northern-Central part of the HCS containing LGM sediment sequences, suggest low productivity (Rein et al., 2005; Salvatteci et al., 2016), which is consistent with the response of the HCS to a weaker Walker circulation. Lastly, the sub-surface waters in the ETSP were more oxygenated during the LGM as a result of increased solubility and to enhanced formation of intermediate waters that can increase the physical supply of oxygen (Meissner et al., 2005). These hydrographic conditions are somewhat similar to El Niño-like conditions with regards to productivity and oxygen, except that SSTs were lower during the LGM and are higher during El Niño events or periods of El Niño like conditions within the Holocene. The results thus confirm that productivity and probably oxygen are more important than temperature (as frequently referred in the literature), for anchovy and oceanic species.

5.2.2 Termination 1

The high inferred abundance of anchovy and mesopelagic fishes and the low inferred abundance of most oceanic species during the Termination 1 could be due to a combination of a slight increase in productivity compared with the LGM and a strong OMZ. Export production in our records (Fig. 8C-E) was relatively low compared with the Holocene values, but during the Termination 1 there was a reduction in the spatial distribution of the main upwelling centers from its modern locations between ~9ºS and ~15ºS to ~9ºS and ~12ºS (Doering et al., 2016). Higher export production values were found between 9ºS and 12ºS and perhaps in this area a higher abundance of anchovy could be found. During the Termination 1 the sea-level was 90 to 120 m below its present level (Fairbanks, 1989), causing changes in the coastline and potential latitudinal shifts in the upwelling centers.

The response of the pelagic fish community off Peru during the Termination 1 could be similar to future warm scenarios that predict an increase in the volume of the OMZ and a decrease in primary production (Brochier et al., 2013; Oerder et al., 2015). The relatively high abundance of anchovy during the Termination 1 could be related to the very strong OMZ, promoting a very thin surface oxygenated habitat and thus concentrating the prey in the upper meters of the water column and limiting the incursion of predators near the coast (Bertrand et al.,

2011). The OMZ among other climatic factors, may be the main reason of relatively high abundance of anchovy. For sardine, the combination of relatively low productivity and strong OMZ seems to be the likely conditions that caused the absence of sardine off Peru. Indeed sardine needs a more oxygenated-deeper habitat to flourish (Bertrand et al., 2011). The lack of sardine scales indicates that sardine was not present (or at very low abundances) during the Termination 1 since preservation was higher (Fig. 8K) and sardine scales are more resistant to degradation. The strong OMZ during the Termination 1 was also unfavorable for jack mackerel and chub mackerel that also need more oxygen to thrive (Bertrand et al., 2016). The low abundance of jack mackerel and chub mackerel, and other predators that cannot cope with low oxygenated waters, can be one of the reason of the increased abundance of mesopelagic fishes. The mesopelagic fishes, could escape from the few predators by resting in the OMZ during the day and, during the night, feed on zooplankton concentrated in the upper meters of the water column.

5.2.3 Holocene

During the Holocene, the high inferred abundance of anchovy, sardine, jack mackerel, chub mackerel, saury, hake and mesopelagic fishes is best explained by an overall increase in productivity compared with the glacial and Termination 1 periods. However, export production and OMZ intensity display strong multi-decadal to centennial-scale changes (Fig. 8A-E), especially during the Late Holocene, that likely affected fish abundances in the HCS. The multidecadal to centennial-scale changes in the inferred abundance of anchovy and other species are also observed in low temporal resolution records from the central HCS (De Vries and Pearcy, 1982).

The new evidence for a strong relationship of anchovy with export production as well as some influence of oxygen can be best interpreted with modern observations of anchovy in the HCS. For anchovy, not only the abundance of food matters but also the type and size of phytoplankton and zooplankton (Espinoza and Bertrand, 2008; Espinoza et al., 2009). High nutrient supply will not only enhance primary productivity but also favor the development of large plankton (e.g. Ayón et al., 2011) that are favorable for particulate feeding anchovy (Espinoza and Bertrand 2008; van der Lingen et al., 2009). The positive relationship of anchovy and the proxy for sub-

surface deoxygenation suggests that a shallow-oxygenated habitat, promoted by a strong OMZ, concentrates the prey near the surface enhancing anchovy foraging and leading to an advantage over other pelagic fishes (Bertrand et al., 2011, 2014). However, during some periods in the Late Holocene characterized by a very strong OMZ, anchovy abundance was not as high as during the CWP (Fig. 8A, F and G) suggesting that a very strong OMZ may not be favorable for anchovy populations. The optimal conditions for anchovy being the current warm period with much of the Holocene also being favorable.

Productivity also seems to be an important factor affecting oceanic species abundance, even if the results are less robust because of the large amount of zeros in the dataset. These zeros likely results from low abundances that cannot be resolved with our sampling resolution as favorable habitat expands and contracts with decadal-scale phenomenon (Bertrand et al., 2004; 2008; 2011, 2016; Gutierrez et al., 2007; Swartzman et al., 2008). However, the higher ratio of oceanic species to anchovy during the Early Holocene suggests that oceanic warm waters intrusion to the coast were considerably more frequent at this time. The Early Holocene was associated with a northward displacement of the ITCZ compared with the Late Holocene and the CWP (Haug et al., 2001). Moreover, during the Early Holocene the ^{14}C reservoir ages showed higher values but also highly variable, suggesting stronger upwelling (Ortlieb et al., 2011). Other globally warm periods were also more favorable while the LGM was unfavorable for these species.

Based on the step-size of our samples, we found no evidence for a negative relationship between hake abundance and the strength of the OMZ (Figs. 11F and 14E). While this result seem at first glance to contradict hake ecology, an important ontogenic characteristic of hake ecology needs to be considered. Juvenile hake present a demersal-pelagic behavior (San Martín et al., 2011) and should not be as dependent on sub-surface oxygenation as adult. It is difficult to differentiate juvenile from adults from hake fish scales in sediment records since they tend to fragment from the sides and thus alter the true widths of the scales. However, Rose (2013) found that most hake scales in Santa Barbara Basin come from juveniles of one to two years of age. We interpret our hake scale record as southward increases in the range of distribution of juvenile hake probably due to an increase in overall productivity during some periods of the Mid and Late Holocene that promoted anchovy development and thus hake given that adult hake prey on

anchovy (Tam et al., 2006). Nonetheless, the more pelagic behavior of juveniles (San Martín et al., 2011), would explain the lack of a relationship between hake scales and oxygen proxies. The abundance of hake is higher in the northern HCS and this is reflected in the higher percentage of hake scales (~16%) in sediment cores collected at ~12ºS (De Vries and Pearcy, 1982) than off Pisco (2.7%, Table 2). Thus, a reconstruction of hake from cores taken further north could reveal changes within the population center of distribution of hake.

A final implication of the record is that the industrial fishery in Peru occurred during the most productive period during the last 25 kyr. Although older parts of the record could have had poorer preservation, the high inferred fish abundance during the last 150 years stems from high fish productivity (PC1, Fig. 14A), and both high fluxes (Fig. 11A) and concentrations (Fig. S1) of anchovy scales. Furthermore, the last 150 years is characterized by records of much higher marine productivity compared with prior periods (Gutierrez et al., 2011; Salvatteci et al., 2014b, 2018) likely due to the combination of a strong and nutrient-rich OMZ (Salvatteci et al., 2014b), strong summer-spring water column stratification promoting diatom blooms (Gutierrez et al., 2011; Salvatteci et al., 2018) and also strong upwelling-favorable winds (Briceño-Zuluaga et al., 2016).

5.3 Implications

The present study provides important insight in the context of climate change. Current models predict a decrease of the productivity in the HCS (Oerder et al., 2015), which would be detrimental for all fish species, and in particular for anchovy. Moreover, a global increase of the OMZ is expected as a consequence of global warming due to lower oxygen dissolution in warmer waters and higher stratification limiting the vertical exchanges (e.g. Schmidtko et al., 2017). Thus the 21st century could thus face conditions alike to those encountered during the Termination 1 period that was characterized by relatively low productivity and an intense OMZ, which might be associated with less anchovy, sardine, and oceanic species in this region (based on Termination 1 period). It is not possible to make any robust prediction at this stage, but our study provide possible scenarios to consider and to test in modelling approaches.

6. Conclusions

Our composite record of fish debris that spans a wide range of climatic and oceanographic conditions reveals the response of fish populations to a unique set of oceanographic end-member conditions and the mechanism driving the temporal changes in fish abundance. Changes in fish scale preservation are not a function of age of sediments, but rather, can be clearly linked to changes in water column oxygenation, and less so to sediment redox conditions. Time-periods characterized by a weak OMZ (i.e. greater oxygenation) like the glacial periods resulted in poor preservation of fish scales. Since scales degrade more easily than vertebrae, we recommend using vertebrae as additional indicators of changes in fish abundance when oxygen concentrations may be higher.

During the last 25 kyr BP, the abundance of anchovy, sardine, jack mackerel, chub mackerel, saury, hake and mesopelagic fishes largely fluctuated at multidecadal to millennial timescales in the HCS. Productivity appears as the primary factor affecting small pelagic fish abundance, though sub-surface oxygenation also affects some species. Anchovy have been the predominant small pelagic fish, at least over centennial to millennial timescales. Its abundance reached a maximum during the Current Warm Period that is characterized by high productivity and intense (but not the most intense) OMZ conditions. Thus, industrial fisheries developed during a period of exceptional productivity in relation to that of the last 25 kyr. The absence of sardine during the glacial periods and the Termination 1 support the hypothesis that sardine need high productivity and oxygen to thrive.

7. Acknowledgements

RS is grateful to the Alexander von Humboldt foundation for granting a postdoctoral fellowship. We acknowledge the Instituto del Mar del Peru (IMARPE) and the joint IMARPE-IRD projects PALEOTRACES and DISCOH for the support of this research. We also acknowledge the program CIENCIACTIVA that granted the research of climate change impacts on the upwelling ecosystem in the frame of the Master's Program in Marine Sciences at the Universidad Peruana Cayetano Heredia. This study was supported by the German Research Foundation through Sonderforschungsbereich 754 ("Climate-Biogeochemistry Interactions in the Tropical Ocean"). SEM observations were performed at the ALYSES facility (IRD, Sorbonne

University, supported by grants from Région Ile-de-France). This paper is dedicated to the memory of Luc Ortlieb and Vicente Ferreira-Bartrina, great scholars, and friends.

8. References

Alegre, A., Bertrand, A., Espino, M., Espinoza, P., Dioses, T., Ñiquen, M., Navarro, I., Simier, M., Ménard, F., 2015. Diet diversity of jack and chub mackerels and ecosystem changes in the northern Humboldt Current system: A long-term study. Progress in Oceanography 137, 299-313.

Ayón, P., Swartzman, G., Espinoza, P., Bertrand, A., 2011. Long-term changes in zooplankton size distribution in the Peruvian Humboldt Current System: conditions favouring sardine or anchovy. Marine Ecology Progress Series 422, 211-222.

Bakun, A., 1990. Global climate change and intensification of coastal upwelling. Science 247, 198-201.

Barange, M., Coetzee, J., Takasuka, A., Hill, K., Gutierrez, M., Oozeki, Y., van der Lingen, C., Agostini, V., 2009. Habitat expansion and contraction in anchovy and sardine populations. Progress in Oceanography 83, 251-260.

Barbraud, C., Bertrand, A., Bouchón, M., Chaigneau, A., Delord, K., Demarcq, H., Gimenez, O., Gutiérrez, M., Gutiérrez, D., Oliveros-Ramos, R., Passuni, G., Tremblay, Y., Bertrand, S., 2018. Density dependence, prey accessibility and prey depletion by fisheries drive Peruvian seabird population dynamics. Ecography, 41, 1092-1102.

Baumgartner, T., Soutar, A., Ferreira-Bartrina, V., 1992. Reconstruction of the history of pacific sardine and northern anchovy populations over the past two millennia from sediments of the Santa Barbara basin, California. CalCOFI Rep. 33, 24-40.

Belmadani, A., Echevin, V., Codron, F., Takahashi, K., Junquas, C., 2014. What dynamics drive future wind scenarios for coastal upwelling off Peru and Chile? Climate Dynamics, 43, 1893-1914.

Bertrand, A., Segura, M., Gutiérrez, M., Vásquez, L., 2004. From small-scale habitat loopholes to decadal cycles: a habitat-based hypothesis explaining fluctuation in pelagic fish populations off Peru. Fish and Fisheries 5, 296-316.

Bertrand, A., Gerlotto, F., Bertrand, S., Gutierrez, M., Alza, L., Chipollini, A., Diaz, E., Espinoza, P., Ledesma, J., Quesquen, R., Peraltilla, S., Chavez, F., 2008. Schooling behaviour

and environmental forcing in relation to anchoveta distribution: An analysis across multiple spatial scales. Progress in Oceanography 79, 264-277.

Bertrand, A., Ballon, M., Chaigneau, A., 2010. Acoustic Observation of Living Organisms Reveals the Upper Limit of the Oxygen Minimum Zone. PLoS ONE, 5, e10330.

Bertrand, A., Chaigneau, A., Peraltilla, S., Ledesma, J., Graco, M., Monetti, F., Chavez, F., 2011. Oxygen: A Fundamental Property Regulating Pelagic Ecosystem Structure in the Coastal Southeastern Tropical Pacific. PLoS ONE 6, e29558.

Bertrand, A., Habasque, J., Hattab, T., Hintzen, N.T., Oliveros-Ramos, R., Gutiérrez, M., Demarcq, H., Gerlotto, F., 2016. 3-D habitat suitability of jack mackerel *Trachurus murphyi* in the Southeastern Pacific, a comprehensive study. Progress in Oceanography 146, 199-211.

Bertrand, A., Grados, D., Colas, F., Bertrand, S., Capet, X., Chaigneau, A., Vargas, G., Mousseigne, A., Fablet, R., 2014. Broad impacts of fine-scale dynamics on seascape structure from zooplankton to seabirds. Nature communications, 5, 5239.

Bertrand, S., Joo, R., Smet, C.A., Tremblay, Y., Barbraud, C., Weimerskirch, H., 2012. Local depletion by a fishery can affect seabird foraging. Journal of Applied Ecology, 49, 1168-1177.

Bertrand A., Völger, R., Defeo O. 2018. Chapter 15: Climate change impacts, vulnerabilities and adaptations: South-West Atlantic and South East Pacific marine fisheries. *In*: Barange, M., Bahri, T., Beveridge, M., Cochrane, K., Funge-Smith, S., Poulain, F. (Eds.) Impacts of Climate Change on fisheries and aquaculture: Synthesis of current knowledge, adaptation and mitigation options. FAO Fisheries Technical Paper 627.

Böning, P., Shaw, T., Pahnke, K., Brumsack, H.J., 2015. Nickel as indicator of fresh organic matter in upwelling sediments. Geochimica et Cosmochimica Acta, 162, 99-108.

Breitburg, D., Levin, L.A., Oschlies, A., Gregoire, M., Chavez, F.P., Conley, D.J., Garcon, V., Gilbert, D., Gutierrez, D., Isensee, K., Jacinto, G.S., Limburg, K.E., Montes, I., Naqvi, S.W.A., Pitcher, G.C., Rabalais, N.N., Roman, M.R., Rose, K.A., Seibel, B.A., Telszewski, M., Yasuhara, M., Zhang, J., 2018. Declining oxygen in the global ocean and coastal waters. Science 359.

Briceño-Zuluaga, F., Sifeddine, A., Caquineau, S., Cardich, J., Salvatteci, R., Gutierrez, D., Ortlieb, L., Velazco, F., Boucher, H., Machado, C., 2016. Terrigenous material supply to the Peruvian central continental shelf (Pisco, 14°S) during the last 1000 years: paleoclimatic implications. Climate of the Past, 12, 787-798.

Brochier, T., Echevin, V., Tam, J., Chaigneau, A., Goubanova, K., Bertrand, A., 2013. Climate change scenarios experiments predict a future reduction in small pelagic fish recruitment in the Humboldt Current system. Global Change Biology 19, 1841-1853.

Brodie, I., Kemp, A.E.S., 1994. Variation in biogenic and detrital fluxes and formation of laminae in late Quaternary sediments from the Peruvian coastal upwelling zone. Marine Geology 116, 385-398.

Carré, M., Sachs, J.P., Purca, S., Schauer, A.J., Braconnot, P., Angeles-Falcón, R., Julien, M., Lavallée, D., 2014. Holocene history of ENSO variance and asymmetry in the eastern tropical Pacific. Science 345, 1045-1048.

Cartes, J.E., Schirone, A., Barsanti, M., Delbono, I., Martínez-Aliaga, A., Lombarte, A., 2017. Recent reconstruction of deep-water macrofaunal communities recorded in Continental Margin sediments in the Balearic Basin. Deep Sea Research Part I: Oceanographic Research Papers, 125, 52-64.

Castillo, R., Gutiérrez, M., Peraltilla, S., Ganoza, F., 2009. Distribución y biomasa de algunos recursos pelágicos peruanos en primavera 2003. Inf. Inst. Mar Perú, 36, 45-51.

Castro, J.J., Santana, A.T., 2000. Synopsis of biological data on the chub mackerel (*Scomber japonicus* Houttuyn, 1782). FAO Fisheries Synopsis 157, 77.

Chavez, F.P., Messié, M., 2009. A comparison of Eastern Boundary Upwelling Ecosystems. Progress in Oceanography 83, 80-96.

Chavez, F., Bertrand, A., Guevara-Carrasco, R., Soler, P., Csirke, J., 2008. The northern Humboldt Current System: Brief history, present status and a view towards the future. Progress in Oceanography 79, 95-105.

Chazen, C.R., Altabet, M.A., Herbert, T.D., 2009. Abrupt mid-Holocene onset of centennial-scale climate variability on the Peru-Chile Margin. Geophysical Research Letters 36, L18704.

Checkley, D., Ayon, P., Baumgartner, T., Bernal, M., Coetzee, J., Emmett, R., Guevara-Carrasco, R., Hutchings, L., Ibaibarriaga, L., Nakata, H., Oozeki, Y., Planque, B., Schweigert, J., Stratoudakis, Y., van der Lingen, C., 2009. Habitats, in: Checkley, D., Alheit, J., Oozeki, Y., Roy, C. (Eds.), Climate Change and Small Pelagic Fish. Cambridge University Press, pp. 12-44.

Chirichigno, N., Cornejo, M., 2001. Catálogo comentado de los peces marinos del Perú. Publicación especial del Instituto del Mar del Perú, 314.

Collette, B.B., 2004. Family Scomberesocidae Müller 1843 -sauries- California Academy of Sciences Annotated Checklists of Fishes 21, 1-6.

Cornejo, R., Koppelmann, R., 2006. Distribution patterns of mesopelagic fishes with special reference to *Vinciguerria lucetia* Garman 1899 (Phosichthyidae: Pisces) in the Humboldt Current Region off Peru. Marine Biology 149, 1519-1537.

Crusius, J., Calvert, S., Pedersen, T., Sage, D., 1996. Rhenium and molybdenum enrichments in sediments as indicators of oxic, suboxic and sulfidic conditions of deposition. Earth and Planetary Science Letters, 145, 65-78.

De Vries, T., Pearcy, W., 1982. Fish debris in sediments of the upwelling zone off central Peru: a late Quaternary record. Deep-Sea Research 28, 87-109.

Diaz-Ochoa, J.A., Lange, C.B., Pantoja, S., De Lange, G.J., Gutierrez, D., Muñoz, P., Salamanca, M., 2008. Fish scales in sediments from off Callao, central Peru. Deep-Sea Research Part II 56, 1124–1135.

Doering, K., Erdem, Z., Ehlert, C., Fleury, S., Frank, M., Schneider, R., 2016. Changes in diatom productivity and upwelling intensity off Peru since the Last Glacial Maximum: Response to basin-scale atmospheric and oceanic forcing. Paleoceanography 31.

Dunn, P.K., Smyth, G.K., 2005. Series evaluation of Tweedie exponential dispersion model densities. Statistics and Computing, 15, 267-280.

Echevin, V., Aumont, O., Ledesma, J., Flores, G., 2008. The seasonal cycle of surface chlorophyll in the Peruvian upwelling system: A modelling study. Progress in Oceanography 79, 167-176.

Erdem, Z., Schönfeld, J., Glock, N., Dengler, M., Mosch, T., Sommer, S., Elger, J., Eisenhauer, A., 2016. Peruvian sediments as recorders of an evolving hiatus for the last 22 thousand years. Quaternary Science Reviews 137, 1-14.

Espino, M., Castillo, R., Fernández, F., 1995. Biology and fisheries of Peruvian hake (*M. gayi peruanus*), in: Alheit, J., Pitcher, T.J. (Eds.), Hake Fisheries, ecology and markets. Chapman & Hall, pp. 339-364.

Espinoza, P., Bertrand, A., 2008. Revisiting Peruvian anchovy (*Engraulis ringens*) trophodynamics provides a new vision of the Humboldt Current system. Progress in Oceanography 79, 215-227.

Espinoza, P., Bertrand, A., van der Lingen, C.D., Garrido, S., Rojas de Mendiola, B., 2009. Diet of sardine (*Sardinops sagax*) in the northern Humboldt Current system and comparison with the diets of clupeoids in this and other eastern boundary upwelling systems. Progress in Oceanography 83, 242-250.

Fairbanks, R.G., 1989. A 17,000-year glacio-eustatic sea level record: influence of glacial melting rates on the Younger Dryas event and deep-ocean circulation. Nature, 342, 637-642.

Feldberg, M.J., Mix, A.C., 2003. Planktonic foraminifera, sea surface temperatures, and mechanisms of oceanic change in the Peru and south equatorial currents, 0-150 ka BP. Paleoceanography, 18, 1016.

Field, D.B., Baumgartner, T.R., Ferreira, V., Gutierrez, D., Lozano-Montes, H., Salvatteci, R., Soutar, A., 2009. Variability from scales in marine sediments and other historical records, in: Checkley, D., Roy, C., Alheit, J., Oozeki, Y. (Eds.), Climate Change and Small Pelagic Fish. Cambridge University Press, pp. 45-63.

Finney, B.P., Alheit, J., Emeis, K.C., Field, D.B., Gutierrez, D., Struck, U., 2010. Paleoecological studies on variability in marine fish populations: A long-term perspective on the impacts of climatic change on marine ecosystems. Journal of Marine Systems 79, 316-326.

Froese, R., Pauly, D., 2018. FishBase. World Wide Web electronic publication. www.fishbase.org.

Ganeshram, R.S., Pedersen, T.F., Calvert, S.E., McNeill, G.W., Fontugne, M.R., 2000. Glacial-interglacial variability in denitrification in the World's Oceans: Causes and consequences. Paleoceanography, 15, 361-376.

Gerlotto, F., Gutierrez, M., Bertrand, A., 2012. Insight on population structure of the Chilean jack mackerel (*Trachurus murphyi*). Aquatic Living Resources 25, 341-355.

Gjøsaeter, J., Kawaguchi, K., 1980. A review of the world resources of mesopelagic fish. No. 193-199. Food & Agriculture Org.

Glantz, S.A., 2002. Primer of Biostatistics, 5th ed. McGraw-Hill.

Goubanova, K., Echevin, V., Dewitte, B., Codron, F., Takahashi, K., Terray, P., Vrac, M., 2011. Statistical downscaling of sea-surface wind over the Peru–Chile upwelling region: diagnosing the impact of climate change from the IPSL-CM4 model. Climate Dynamics 36, 1365-1378.

Guevara-Carrasco, R., Lleonart, J., 2008. Dynamics and fishery of the Peruvian hake: Between nature and man. Journal of Marine Systems 71, 249-259.

Guiñez, M., Valdés, J., Sifeddine, A., Boussafir, M., Dávila, P., 2014. Anchovy population and ocean-climatic fluctuations in the Humboldt Current System during the last 700 years and their implications. Paleogeography, Paleoclimatology, Palaeoecology 415, 210-224.

Gutierrez, M., Swartzman, G., Bertrand, A., Bertrand, S., 2007. Anchovy (*Engraulis ringens*) and sardine (*Sardinops sagax*) spatial dynamics and aggregation patterns in the Humboldt Current ecosystem, Peru, from 1983–2003. Fish Oceanogr. 16, 155-168.

Gutierrez, D., Sifeddine, A., Field, D.B., Ortlieb, L., Vargas, G., Chavez, F., Velazco, F., Ferreira, V., Tapia, P., Salvatteci, R., Boucher, H., Morales, M.C., Valdes, J., Reyss, J.L., Campusano, A., Boussafir, M., Mandeng-Yogo, M., Garcia, M., Baumgartner, T., 2009. Rapid reorganization in ocean biogeochemistry off Peru towards the end of the Little Ice Age. Biogeosciences 6, 835-848.

Gutierrez, D., Bouloubassi, I., Sifeddine, A., Purca, S., Goubanova, K., Graco, M., Field, D., Méjanelle, L., Velazco, F., Lorre, A., Salvatteci, R., Quispe, D., Vargas, G., Dewitte, B., Ortlieb, L., 2011. Coastal cooling and increased productivity in the main upwelling zone off Peru since the mid-twentieth century. Geophysical Research Letters 38, L07603.

Gutierrez, M., Castillo, R., Segura, M., Peraltilla, S., Flores, M., 2012. Trends in spatio-temporal distribution of Peruvian anchovy and other small pelagic fish biomass from 1966-2009. Latin american journal of aquatic research 40, 633-648.

Haug, G.H., Hughen, K.A., Sigman, D.M., Peterson, L.C., Rohl, U., 2001. Southward Migration of the Intertropical Convergence Zone Through the Holocene. Science 293, 1304-1308.

Herring, P., 2001. The biology of the deep ocean. OUP Oxford.

Hopkins, T.L., Baird, R.C., 1985. Aspects of the Trophic Ecology of the Mesopelagic Fish *Lampanyctus alatus* (Family Myctophidae) in the Eastern Gulf of Mexico. Biological Oceanography, 3, 285-313.

Hutchinson, J.J., Trueman, C.N., 2006. Stable isotope analyses of collagen in fish scales: limitations set by scale architecture. Journal of Fish Biology 69, 1874-1880.

Irigoien, X., Klevjer, T.A., Rostad, A., Martinez, U., Boyra, G., Acuna, J.L., Bode, A., Echevarria, F., Gonzalez-Gordillo, J.I., Hernandez-Leon, S., Agusti, S., Aksnes, D.L., Duarte, C.M., Kaartvedt, S., 2014. Large mesopelagic fishes biomass and trophic efficiency in the open ocean. Nat Commun 5, 3271.

Jaccard, S.L., Galbraith, E.D., 2012. Large climate-driven changes of oceanic oxygen concentrations during the last deglaciation. Nature geoscience 5, 151-156.

Jaccard, S.L., Galbraith, E.D., Frölicher, T.L., Gruber, N., 2014. Ocean (de)oxygenation across the last deglaciation: Insights for the future. Oceanography 27, 26-35.

Jahncke, J., Goya, E., 1998. Las dietas del guanay y piquero peruano como indicadoras de la abundancia y distribucion de anchoveta. Boletin del Instituto del Mar del Peru 17, 15-34.

Joo, R., Bertrand, A., Bouchon, M., Chaigneau, A., Demarcq, H., Tam, J., Simier, M., Gutiérrez, D., Gutiérrez, M., Segura, M., Fablet, R., Bertrand, S., 2014. Ecosystem scenarios shape fishermen spatial behavior. The case of the Peruvian anchovy fishery in the Northern Humboldt Current System. Progress in Oceanography, 128, 60-73.

Jordán, R., Csirke, J., Tsukayama, I., 1978. Situación de los recursos anchoveta, sardina, jurel y caballa a junio 1978. Instituo del Mar del Peru Informe No. 56, 32.

Kaartvedt, S., Røstad, A., Klevjer, T.A., Staby, A., 2009. Use of bottom-mounted echo sounders in exploring behavior of mesopelagic fishes. Marine Ecology Progress Series, 395, 109-118.

Karstensen, J., Stramma, L., Visbeck, M., 2008. Oxygen minimum zones in the eastern tropical Atlantic and Pacific oceans. Progress in Oceanography 77, 331-350.

Koutavas, A., Joanides, S., 2012. El Niño–Southern Oscillation extrema in the Holocene and Last Glacial Maximum. Paleoceanography 27.

Koutavas, A., Lynch-Stieglitz, J., Marchitto, T.M., Sachs, J.P., 2002. El Niño-like pattern in ice age tropical Pacific sea surface temperature. Science 297, 226-230.

Koutavas, A., Lynch-Stieglitz, J., 2004. Variability of the marine ITCZ over the eastern Pacific during the past 30,000 years. In E.F. Diaz, R.S. Bradley (Eds.), The Hadley Circulation: Present Past and Future. Dortrechts: Springer Academic Publishers.

Kuwae, M., Yamamoto, M., Sagawa, T., Ikehara, K., Irino, T., Takemura, K., Takeoka, H., Sugimoto, T., 2017. Multidecadal, centennial, and millennial variability in sardine and anchovy abundances in the western North Pacific and climate–fish linkages during the late Holocene. Progress in Oceanography, 159, 86-98.

Levin, L.A., 2018. Manifestation, Drivers, and Emergence of Open Ocean Deoxygenation. Annual Review of Marine Science 10, 229-260.

Lozano-Montes, H., 1997. Reconstruction of marine fish populations using fossil fish scales deposited in Santa Barbara Basin (USA). Centro de Investigación Científica y de Educación Superior de Ensenada, p. 97.

Mayewski, P.A., Rohling, E.E., Stager, J.C., Karlén, W., Maasch, K.A., Meeker, L.D., Meyerson, E.A., Gasse, F., van Kreveld, S., Holmgren, K., Lee-Thorp, J., Rosqvist, G., Rack, F., Staubwasser, M., Schneider, R., Steig, E.J., 2004. Holocene climate variability. Quaternary Research, 62, 243-255.

Meissner, K.J., Galbraith, E.D., Völker, C., 2005. Denitrification under glacial and interglacial conditions: A physical approach. Paleoceanography, 20, PA3001.

Mix, A.C., Bard, E., Schneider, R., 2001. Environmental processes of the ice age: land, oceans, glaciers (EPILOG). Quaternary Science Reviews 20, 627-657.

Nelson, J.S., 2006. Fishes of the World. Wiley

O'Connell, J.M., Tunnicliffe, V., 2001. The use of sedimentary fish remains for interpretation of long-term fish population fluctuations. Marine Geology 174, 177-195.

Oerder, V., Colas, F., Echevin, V., Codron, F., Tam, J., Belmadani, A., 2015. Peru-Chile upwelling dynamics under climate change. Journal of Geophysical Research: Oceans, 120, 1152-1172.

Ortlieb, L., Vargas, G., Saliège, J.-F., 2011. Marine radiocarbon reservoir effect along the northern Chile-southern Peru coast (14-24°S) throughout the Holocene. Quaternary Research 75, 91-103.

Patterson, R.T., Wright, C., Chang, A.S., Taylor, L.A., Lyons, P.D., Dallimore, A., Kumar, A., 2011. Atlas of common squamatological (fish scale) material in coastal British Columbia and an assessment of the utility of various scale types in paleofisheries reconstruction. Palaeontologia Electronica 4, 88.

Pauly, D., Tsukayama, I., 1987. On the implementation of management-oriented fishery research: the case of the Peruvian anchoveta. ICLARM Studies and Reviews, in: Pauly, D., Tsukayama, I. (Eds.), The Peruvian Anchoveta and its upwelling ecosystem: three decades of change. Instituto del Mar del Peru (IMARPE), Deutsche Gesellschaft fur Technische Zusammenarbeit (GTZ) and International Center for Living Aquatic Resources Management (ICLARM), pp. 1-13.

Pedro, J.B., Bostock, H.C., Bitz, C.M., He, F., Vandergoes, M.J., Steig, E.J., Chase, B.M., Krause, C.E., Rasmussen, S.O., Markle, B.R., Cortese, G., 2015. The spatial extent and dynamics of the Antarctic Cold Reversal. Nature Geoscience 9, 51-55.

Prince, E.D., Goodyear, C.P., 2006. Hypoxia-based habitat compression of tropical pelagic fishes. Fisheries Oceanography, 15, 451-464.

Rein, B., Lückge, A., Reinhardt, L., Sirocko, F., Wolfe, A., Dullo, W.-C., 2005. El Niño variability off Peru during the last 20,000 years. Paleoceanography 20, PA4003.

Rose, K. M., 2013. Fish Scales and Skeletal Debris as Indicators of Changes in Small Pelagic Fishes in the Santa Barbara Basin: Fishing or Natural Variability?. Hawai'i Pacific University. Master of Science in Marine Science: 184.

Salvatteci, R., Field, D.B., Baumgartner, T., Ferreira, V., Gutierrez, D., 2012. Evaluating fish scale preservation in sediment records from the oxygen minimum zone off Peru. Paleobiology 38, 52-78.

Salvatteci, R., Field, D., Sifeddine, A., Ortlieb, L., Ferreira, V., Baumgartner, T., Caquineau, S., Velazco, F., Reyss, J.L., Sanchez-Cabeza, J.A., Gutierrez, D., 2014a. Cross-stratigraphies from a seismically active mud lens off Peru indicate horizontal extensions of laminae, missing sequences, and a need for multiple cores for high resolution records. Marine Geology 357, 72-89.

Salvatteci, R., Gutierrez, D., Field, D., Sifeddine, A., Ortlieb, L., Bouloubassi, I., Boussafir, M., Boucher, H., Cetin, F., 2014b. The response of the Peruvian Upwelling Ecosystem to centennial-scale global change during the last two millennia. Climate of the Past 10, 715-731.

Salvatteci, R., Gutierrez, D., Sifeddine, A., Ortlieb, L., Druffel, E., Boussafir, M., Schneider, R., 2016. Centennial to millennial-scale changes in oxygenation and productivity in the Eastern Tropical South Pacific during the last 25 000 years. Quaternary Science Reviews 131, 102-117.

Salvatteci, R., Field, D., Gutiérrez, D., Baumgartner, T., Ferreira, V., Ortlieb, L., Sifeddine, A., Grados, D., Bertrand, A., 2018. Multifarious anchovy and sardine regimes in the Humboldt Current System during the last 150 years. Global Change Biology 24, 1055-1068.

Salvatteci, R., Schneider, R.; Blanz, T.; Mollier-Vogel E. 2019. Deglacial to Holocene Ocean Temperatures in the Humboldt Current System as Indicated by Alkenone Paleothermometry. Geophysical Research Letters 46, doi: 10.1029/2018gl080634

San Martín, M.A., Cubillos, L., Saavedra, J.C., 2011. The spatio-temporal distribution of juvenile hake (*Merluccius gayi gayi*) off central southern Chile (1997–2006). Aquatic Living Resources 24, 161-168.

Schmidtko, S., Stramma, L., Visbeck, M., 2017. Decline in global oceanic oxygen content during the past five decades. Nature 542, 335-339.

Scholz, F., McManus, J., Mix, A., Hensen, C., Schneider, R., 2014. The impact of ocean deoxygenation on the ocean's iron supply. Nature Geoscience 7, 433-437.

Shackleton, L.Y., Johnson, R.F., 1988. Identification of and distinction between the scales of south african pilchard *Sardinops ocellatus* and cape anchovy *Engrauilis capensis*. South African Journal of Marine Science 6, 207-216.

Shackleton, L.Y., 1988. Scale shedding: an important factor in fossil fish studies. ICES Journal of Marine Science 44, 259-263.

Sibert, E.C., Hull, P.M., Norris, R.D., 2014. Resilience of Pacific pelagic fish across the Cretaceous/Palaeogene mass extinction. Nature geoscience, 7, 667-670.

Sibert, E.C., Norris, R.D., 2015. New Age of Fishes initiated by the Cretaceous-Paleogene mass extinction. Proc Natl Acad Sci U S A, 112, 8537-8542.

Skilbeck, C.G., Fink, D., 2006. Data report: Radiocarbon dating and sedimentation rates for Holocene–upper Pleistocene sediments, eastern equatorial Pacific and Peru continental margin, in: Jorgensen, B.B., D'Hondt, S.L., Miller, D.J. (Eds.), Proc. ODP, Sci. Results, 201, 1–15.

Skrivanek, A., Hendy, I.L., 2015. A 500 year climate catch: Pelagic fish scales and paleoproductivity in the Santa Barbara Basin from the Medieval Climate Anomaly to the Little Ice Age (AD 1000–1500). Quaternary International 387, 36-45.

Soutar, A., Isaacs, J., 1974. Abundance of pelagic fish during the 19th and 20th century as recorded in anaerobic sediment off the Californias. Fisheries Bulletin 72, 257-273.

Stramma, L., Johnson, G.C., Sprintall, J., Mohrholz, V., 2008. Expanding Oxygen-Minimum Zones in the Tropical Oceans. Science 320, 655-658.

Stramma, L., Prince, E.D., Schmidtko, S., Luo, J., Hoolihan, J.P., Visbeck, M., Wallace, D.W.R., Brandt, P., Körtzinger, A., 2012. Expansion of oxygen minimum zones may reduce available habitat for tropical pelagic fishes. Nature climate change, 2, 33-37.

Struck, U., Altenbach, A.V., Emeis, K.C., Alheit, J., Eichner, C., Schneider, R., 2002. Changes of the upwelling rates of nitrate preserved in the $\delta^{15}N$-signature of sediments and fish scales from the diatomaceous mud belt of Namibia. Geobios 35, 3-11.

Swartzman, G., Bertrand, A., Gutiérrez, M., Bertrand, S., Vasquez, L., 2008. The relationship of anchovy and sardine to water masses in the Peruvian Humboldt Current System from 1983 to 2005. Progress in Oceanography 79, 228-237.

Sydeman, W.J., Garcia-Reyes, M., Schoeman, D.S., Rykaczewski, R.R., Thompson, S.A., Black, B.A., Bograd, S.J., 2014. Climate change and wind intensification in coastal upwelling ecosystems. Science 345, 77-80.

Tam, J., Purca, S., Duarte, L.O., Blaskovic, V., Espinoza, P., 2006. Changes in the diet of hake associated with El Niño 1997–1998 in the northern Humboldt Current ecosystem. Advances in Geosciences 6, 63-67.

Tribovillard, N., Algeo, T.J., Lyons, T., Riboulleau, A., 2006. Trace metals as paleoredox and paleoproductivity proxies: An update. Chemical Geology, 232, 12-32.

Valdés, J., Ortlieb, L., Gutierrez, D., Marinovic, L., Vargas, G., Sifeddine, A., 2008. 250 years of sardine and anchovy scale deposition record in Mejillones Bay, northern Chile. Progress in Oceanography 79, 198-207.

van der Lingen, C.D., Bertrand, A., Bode, A., Brodeur, R., Cubillos, L.A., Espinoza, P., Friedland, K., Garrido, S., Irigoien, X., Miller, T., Möllmann, C., Rodriguez-Sanchez, R., Tanaka, H., Temming, A., 2009. Trophic dynamics. In D. Checkley, J. Alheit, Y. Oozeki, C. Roy (Eds.), Climate Change and Small Pealgic Fish (pp. 112-157): Cambridge University Press.

Wang, D., Gouhier, T.C., Menge, B.A., Ganguly, A.R., 2015. Intensification and spatial homogenization of coastal upwelling under climate change. Nature 518, 390-394.

Wisshak, M., Tribollet, A., Golubic, S., Jakobsen, J., Freiwald, A., 2011. Temperate bioerosion: ichnodiversity and biodiversity from intertidal to bathyal depths (Azores). Geobiology 9, 492-520.

TABLES AND FIGURES

Fish debris in sediments from the last 25 kyr in the Humboldt Current reveal the role of productivity and oxygen on small pelagic fishes

Salvatteci, R.[1]; Gutierrez, D.[2,3]; Field, D.[4]; Sifeddine, A.[5,6]; Ortlieb, L.[5†]; Caquineau, S.[5]; Baumgartner, T.[7]; Ferreira, V.[7†]; Bertrand, A.[8]

[1]Institute of Geosciences, Kiel University, Kiel, Germany

[2]Instituto del Mar del Perú (IMARPE), Esquina Gamarra y General Valle s/n, Callao, Perú

[3] Programa de Maestría de Ciencias del Mar, Facultad de Ciencias y Filosofía, Universidad Peruana Cayetano Heredia, Lima, Perú

[4]College of Natural Sciences, Hawaii Pacific, University, Kaneohe, HI, USA

[5]Institut de Recherche pour le Développement (IRD)-Sorbonne Universités (UPMC, Univ. Paris 06)-CNRS-MNHN, LOCEAN Laboratory, Center IRD France-Nord, Bondy, France

[6]Departamento de Geoquímica, LMI PALEOTRACES (IRD, UPMC, UFF, Uantof, UPCH), Universidade Federal Fluminense, Niteroi, RJ, Brazil

[7]Centro de Investigación Científica y de Educación Superior de Ensenada, Ensenada, Baja California C.P, México

[8]IRD, UMR MARBEC, IRD/IFREMER/ CNRS/UM, Séte, France

[†]Deceased.

TABLES

Table 1. Relative abundance of the different fish debris types in the composite record B14-G10-G14

Fish debris type	Number of debris	%
Fish scales from all species	13934	11.9
Fish scale fragments	72122	61.5
Spines	12831	10.9
Spine fragments	2908	2.5
Vertebrae	3869	3.3
Other bones	11177	9.5
Jaws	468	0.4
	117309	

Table 2. Relative abundance of the fish scales from different fish species in the composite record B14-G10-G14

Fish species/group	Number of scales	%
Anchovy	12486	89.6
Sardine	177	1.27
Jack mackerel	150	1.08
Chub mackerel	34	0.24
Saury	35	0.25
Hake	379	2.72
Mesopelagic fishes	410	2.94
Unidentified	263	1.89
	13934	

Table 3. Spearman correlation values (r_s) between the different types of fish debris fluxes from the composite record B14-G10-G14. Underlined values indicate significant values after correcting for multiple comparisons ($p<0.002$). The asterisks at the right side of some values indicate that the r_s value was obtained from two categories that share the same data (e.g. all species scales and anchovy scales).

	All fish scales (n=317)	Anchovy scales (n=317)	Sardine scales (n=317)	Jack mackerel scales (n=317)	Chub mackerel scales (n=317)	Saury scales (n=317)	Hake scales (n=317)	Mesopelagic fish scales (n=317)	Unidentified fish scales (n=317)	Scale fragments (n=317)	All bones (spines + vertebrae + other bones) (n=317)	Anchovy vertebrae (n=317)	Other vertebrae (n=317)	Bones (n=317)	Jaws (n=293)	Spines (n=317)	Spine fragments (n=317)	Integrity index (n=305)	Bio-erosion index (n=310)	Scales to vertebrae (n=310)	Compound preservation index (n=311)	$\delta^{15}N$ (n=241)	Mo/Re (n=315)	Ni EF (n=313)	TOC (n=245)	$CaCO_3$ (n=286)
All fish scales	1.00																									
Anchovy scales	0.97*	1.00																								
Sardine scales	0.25*	0.21	1.00																							
Jack mackerel scales	0.16*	0.04	0.17	1.00																						
Chub mackerel scales	0.23*	0.17	0.21	0.24	1.00																					
Saury scales	0.20*	0.18	0.08	0.13	0.15	1.00																				
Hake scales	0.34*	0.27	0.08	0.11	0.17	0.13	1.00																			
Mesopelagic fish scales	0.37*	0.25	0.11	0.29	0.13	0.14	0.16	1.00																		
Unidentified fish scales	0.17*	0.07	0.10	0.21	0.24	0.08	0.17	0.13	1.00																	
Scale fragments	0.86	0.89	0.24	0.06	0.17	0.13	0.23	0.21	0.06	1.00																
All bones	0.62	0.61	0.21	0.25	0.15	0.10	0.17	0.27	0.04	0.75	1.00															
Anchovy vertebrae	0.40	0.42	0.15	0.16	0.11	0.02	0.01	0.11	0.00	0.56	0.76*	1.00														
Other vertebrae	0.38	0.30	0.21	0.35	0.15	0.11	0.25	0.40	0.16	0.34	0.58*	0.36	1.00													
Bones	0.52	0.52	0.15	0.19	0.09	0.08	0.15	0.23	0.01	0.65	0.92*	0.68	0.52	1.00												
Jaws	0.46	0.44	0.09	0.13	0.02	0.04	0.21	0.17	-0.07	0.54	0.65*	0.50	0.43	0.61	1.00											
Spines	0.66	0.67	0.25	0.20	0.17	0.11	0.16	0.24	0.05	0.79	0.94*	0.71	0.47	0.77	0.57	1.00										
Spine fragments	0.43	0.43	0.13	0.17	0.10	0.00	0.09	0.17	-0.01	0.58	0.80*	0.61	0.34	0.73	0.52	0.71	1.00									
Integrity index	0.20	0.09	0.04	0.23	0.15	0.16	0.20	0.36	0.18	0.06	0.00	-0.10	0.10	-0.02	0.02	-0.01	-0.04	1.00								
Bio-erosion index	0.29	0.26	0.03	-0.01	0.11	0.13	0.15	0.16	0.18	0.12	-0.09	-0.20	0.04	-0.12	-0.06	-0.02	-0.20	0.19	1.00							
Scales to vertebrae	0.55*	0.55*	0.10*	-0.11*	0.11*	0.12*	0.22*	0.08*	0.13*	0.35	-0.10*	-0.29*	-0.36*	-0.14	-0.08	0.04	-0.08	0.18	0.32	1.00						
Compound preservation index	0.37	0.30	0.06	0.07	0.15	0.20	0.19	0.26	0.22	0.17	-0.12	-0.27	-0.11	-0.13	-0.06	-0.06	-0.15	0.67*	0.69*	0.55*	1.00					
$\delta^{15}N$	0.39	0.39	0.08	0.06	0.10	0.17	0.02	0.19	0.14	0.28	0.03	-0.02	-0.06	-0.03	0.03	0.12	-0.06	0.24	0.44	0.47	0.55	1.00				
Mo/Re	0.16	0.15	0.22	0.14	0.18	0.03	-0.06	0.18	0.09	0.15	-0.03	0.03	-0.03	-0.10	-0.08	0.05	-0.13	0.22	0.11	0.22	0.22	0.40	1.00			
Ni EF	0.38	0.36	0.42	0.24	0.26	0.02	0.13	0.23	0.04	0.41	0.38	0.35	0.31	0.23	0.21	0.43	0.27	0.09	-0.05	0.09	0.06	0.18	0.44	1.00		
TOC	0.40	0.39	0.25	0.14	0.17	0.03	0.16	0.20	0.02	0.44	0.56	0.38	0.44	0.51	0.39	0.53	0.45	-0.07	-0.17	-0.03	-0.17	-0.08	-0.13	0.40	1.00	
$CaCO_3$	0.29	0.29	0.01	0.05	0.10	0.10	-0.06	0.16	0.14	0.22	0.22	0.10	0.13	0.26	0.14	0.21	0.08	0.13	0.16	0.16	0.17	0.42	0.05	-0.13	0.30	1.00

Table 4. Spearman correlation values (r_s) between the different types of fish scales and vertebrae fluxes in the well-preserved samples from the composite record B14-G10-G14. The number of samples for each component is indicated between parentheses. Underlined values indicate significant values after correcting for multiple comparisons ($p<0.002$). The asterisks at the right side of some values indicate that the r_s value was obtained from two categories that share the same data (e.g. all species scales and anchovy scales).

	All fish scales (n=135)	Anchovy scales (n=135)	Sardine scales (n=135)	Jack mackerel scales (n=135)	Chub mackerel scales (n=135)	Saury scales (n=135)	Hake scales (n=135)	Mesopelagic fish scales (n=135)	Unidentified fish scales (n=135)	Scale fragments (n=135)	All bones (spines + vertebrae + other bones) (n=135)	Anchovy vertebrae (n=135)	Other vertebrae (n=135)	Bones (n=135)	Jaws (n=123)	Spines (n=135)	Spine fragments (n=135)	Integrity index (n=132)	Bio-erosion index (n=135)	Scales to vertebrae (n=135)	Compound preservation index (n=135)	$\delta^{15}N$ (n=112)	Mo/Re (n=135)	Ni EF (n=135)	TOC (n=112)	$CaCO_3$ (n=128)
All fish scales	1.00																									
Anchovy scales	0.95*	1.00																								
Sardine scales	0.24	0.20	1.00																							
Jack mackerel scales	0.16*	-0.01	0.15	1.00																						
Chub mackerel scales	0.19*	0.10	0.21	0.34	1.00																					
Saury scales	0.20*	0.17	0.13	0.08	0.05	1.00																				
Hake scales	0.31*	0.21	0.10	0.23	0.20	0.11	1.00																			
Mesopelagic fish scales	0.28*	0.12	0.15	0.38	0.21	0.20	0.18	1.00																		
Unidentified fish scales	0.26*	0.11	0.11	0.25	0.30	0.05	0.28	0.29	1.00																	
Scale fragments	0.84*	0.89	0.24	0.01	0.13	0.12	0.18	0.09	0.07	1.00																
All bones	0.62	0.60	0.27	0.35	0.19	0.15	0.11	0.30	0.02	0.72	1.00															
Anchovy vertebrae	0.40	0.44	0.18	0.21	0.15	0.14	-0.06	0.10	-0.04	0.57	0.70*	1.00														
Other vertebrae	0.36	0.26	0.25	0.47	0.19	0.13	0.24	0.51	0.20	0.29	0.55*	0.21	1.00													
Bones	0.56	0.56	0.20	0.23	0.13	0.11	0.11	0.25	0.03	0.64	0.90*	0.58	0.48	1.00												
Jaws	0.47	0.42	0.13	0.16	0.05	0.12	0.13	0.18	-0.06	0.47	0.61*	0.39	0.32	0.57	1.00											
Spines	0.63	0.64	0.29	0.28	0.19	0.15	0.09	0.24	0.01	0.74	0.93*	0.67	0.43	0.74	0.52	1.00										
Spine fragments	0.40	0.37	0.18	0.32	0.17	0.01	0.02	0.13	-0.03	0.52	0.75*	0.55	0.32	0.63	0.48	0.67	1.00									
Integrity index	-0.12	-0.21	-0.08	0.23	0.14	0.10	0.08	0.17	0.16	-0.21	-0.10	-0.08	0.16	-0.10	-0.08	-0.18	-0.12	1.00								
Bio-erosion index	0.11	0.09	-0.09	-0.09	-0.01	-0.01	0.06	0.10	0.15	-0.07	-0.16	-0.15	-0.02	-0.10	-0.09	-0.15	-0.29	0.00	1.00							
Scales to vertebrae	0.43*	0.43*	-0.00*	-0.26*	0.01*	-0.06*	0.22*	-0.11*	0.21*	0.25*	-0.13*	-0.25*	-0.40*	-0.08	-0.07	-0.02	-0.12	-0.17	0.10	1.00						
Compound preservation index	0.12	0.09	-0.15	-0.16	-0.02	0.07	0.03	-0.03	0.20	-0.11	-0.32	-0.32	-0.29	-0.23	-0.15	-0.28	-0.37	0.32*	0.59*	0.49*	1.00					
$\delta^{15}N$	0.34	0.38	-0.07	-0.21	0.05	0.08	-0.14	0.12	0.06	0.22	0.04	0.03	-0.06	0.07	0.05	0.09	-0.07	-0.04	0.38	0.32	0.44	1.00				
Mo/Re	0.14	0.17	0.28	0.07	0.27	-0.03	0.05	0.12	0.14	0.19	0.07	0.20	0.04	-0.06	-0.22	0.18	-0.06	0.19	-0.11	0.12	-0.01	0.25	1.00			
Ni EF	0.26	0.27	0.45	0.16	0.31	0.03	0.12	0.20	0.00	0.38	0.35	0.36	0.24	0.15	0.11	0.43	0.27	-0.03	-0.29	-0.01	-0.25	-0.05	0.61	1.00		
TOC	0.51	0.46	0.25	0.22	0.28	0.10	0.23	0.27	0.13	0.50	0.55	0.27	0.44	0.42	0.45	0.56	0.37	-0.14	-0.13	0.12	-0.23	0.03	-0.06	0.31	1.00	
$CaCO_3$	0.37	0.37	0.02	-0.05	0.16	0.10	0.00	0.12	0.28	0.25	0.21	0.08	0.11	0.29	0.15	0.20	-0.06	0.06	0.23	0.27	0.27	0.60	0.07	-0.20	0.36	1.00

FIGURES

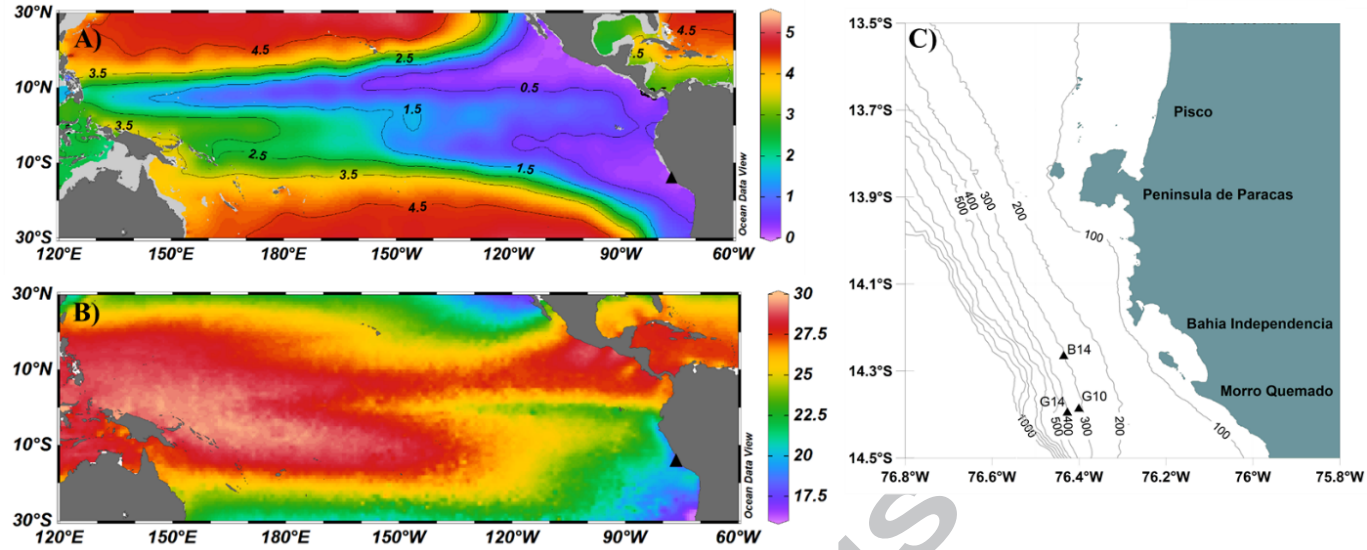

Figure 1. A) Dissolved oxygen content (mL x L^{-1}) at 300 meters depth in the Tropical Pacific. B) Sea Surface temperature (ºC) plot over the Tropical Pacific. The black triangles in A and B indicate the location of the composite record (B14-G10-G14) used in this study. C) Detailed map of the position of cores B14, G10 and G14 used to assemble the composite record.

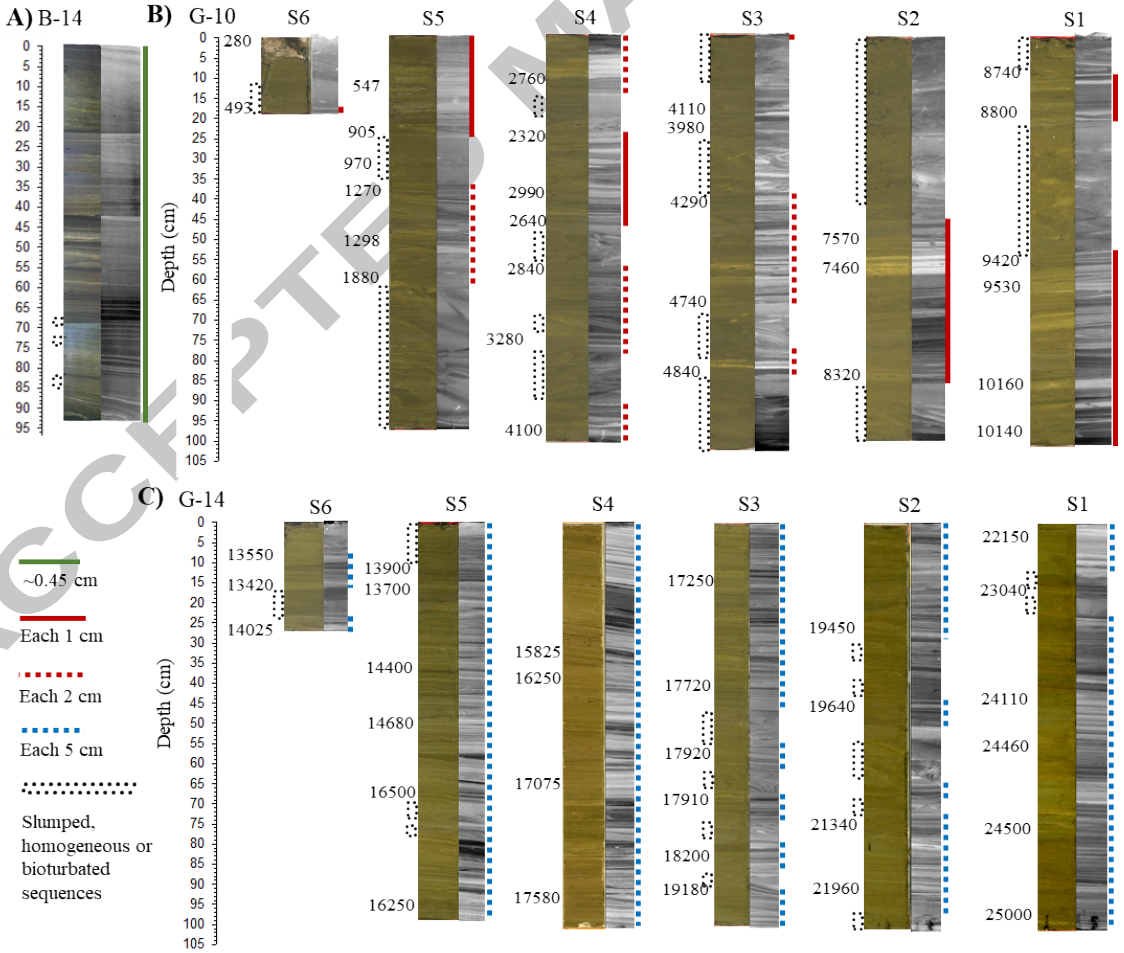

Figure 2. Photographs and X-ray images of the sediment cores used to assemble the composite record. A) Box-core B05-14. B) Gravity core G-10. C) Gravity G-14. Cores G-10 and G-14 were divided onboard into 6 sections (S1 to S6), where S6 is the most recent section. Numbers at the left side of the photographs represent ^{14}C years cal BP. Modified from Salvatteci et al. (2014b; 2016).

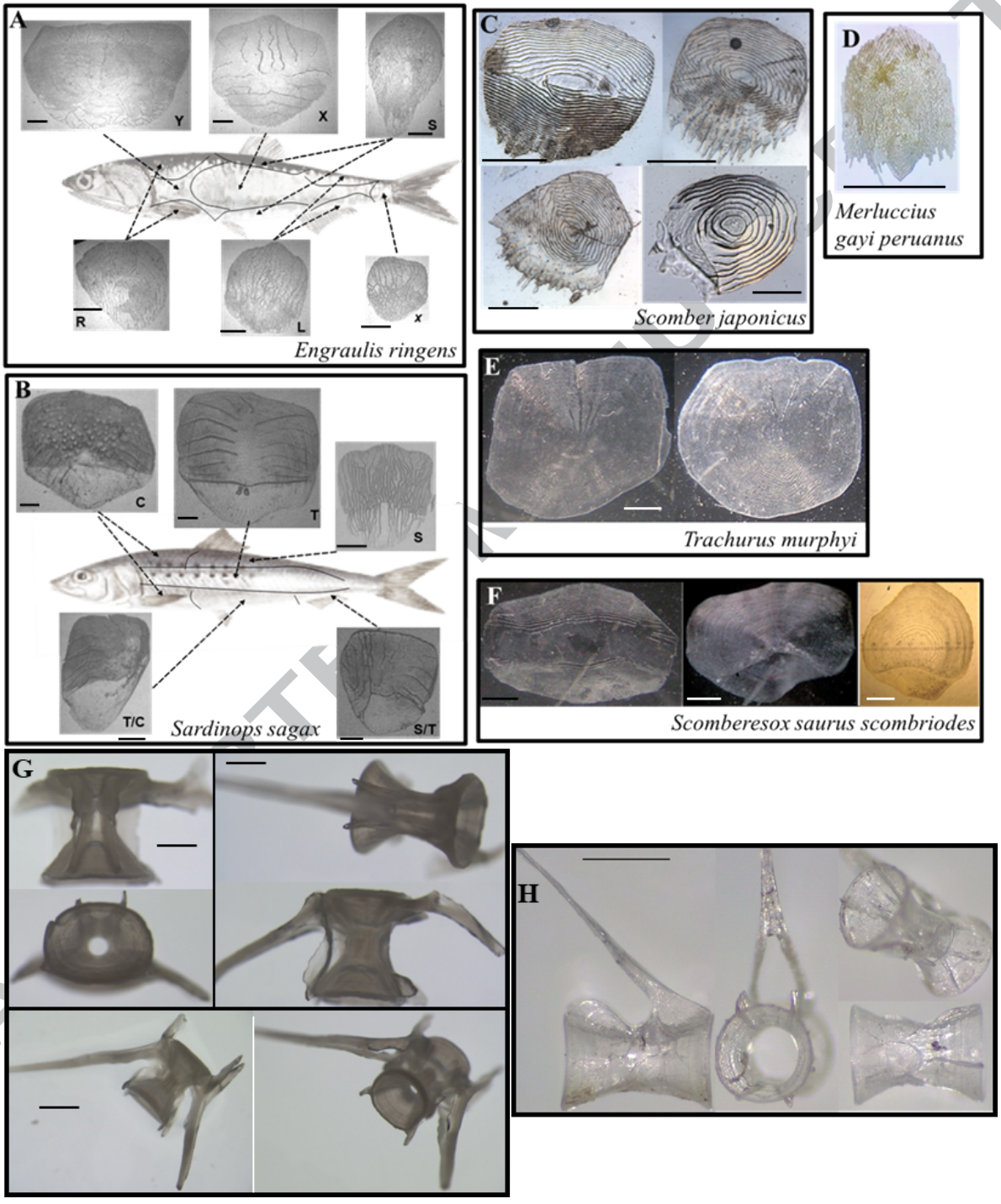

Figure 3. Fish debris from the most abundant and commercially important fishes in the Humboldt Current System taken from recently caught fishes. A) Fish scales from anchovy (*Engraulis ringens*) taken from

different regions of fish. B) Fish scales from sardine (*Sardinops sagax*) taken from different regions of fish. The nomenclature of the scale types (Y, X, S, R, L, and x for anchovy and C, T, S, T/C and S/T for sardine) are after Shackleton and Johnson (1988) and Lozano-Montes (1997). C) Different scale types from chub mackerel (*Scomber japonicus*). D) Typical fish scale of hake (*Merluccius gayi peruanus*). E) Fish scales from jack mackerel (*Trachurus murphyi*). F) Three different fish scales from saury (*Scomberesox saurus scombriodes*). G) Different types of anchovy vertebrae. H) Different types of *Vincinguerria lucetia* vertebrae. Horizontal scale bar = 1mm.

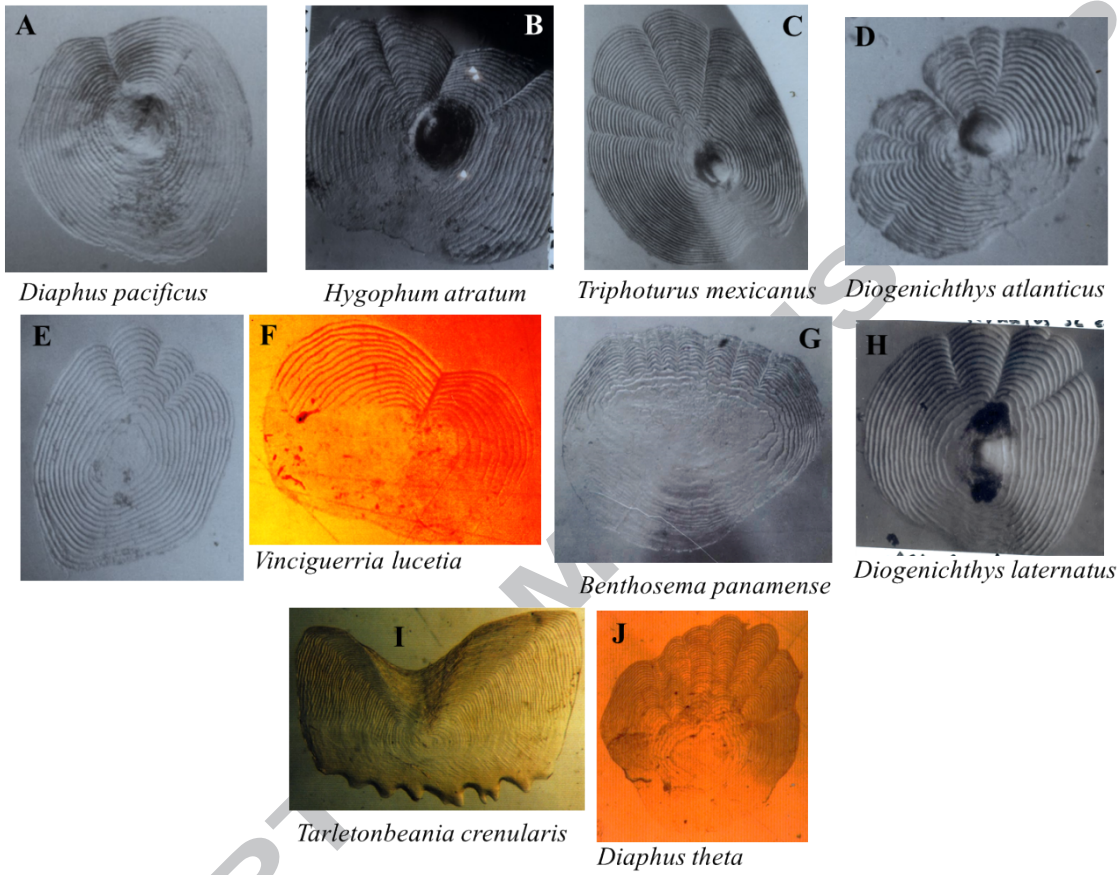

Figure 4. Fish scale of some mesopelagic fishes. A) *Diaphus pacificus*. B) *Hygophum atratum*. C) *Triphoturus mexicanus*. D) *Diogenichthys atlanticus*. E) and F) *Vinciguerria lucetia*. G) *Benthosema panamense*. H) *Diogenichthys laternatus*. I) *Tarletonbeania crenularis*. J) *Diaphus theta*. Images taken from the fish scale collection of CICESE. Scale widths were not measured but based on observation from the sediment records the scale diameters range from 0.5 to 2 mm.

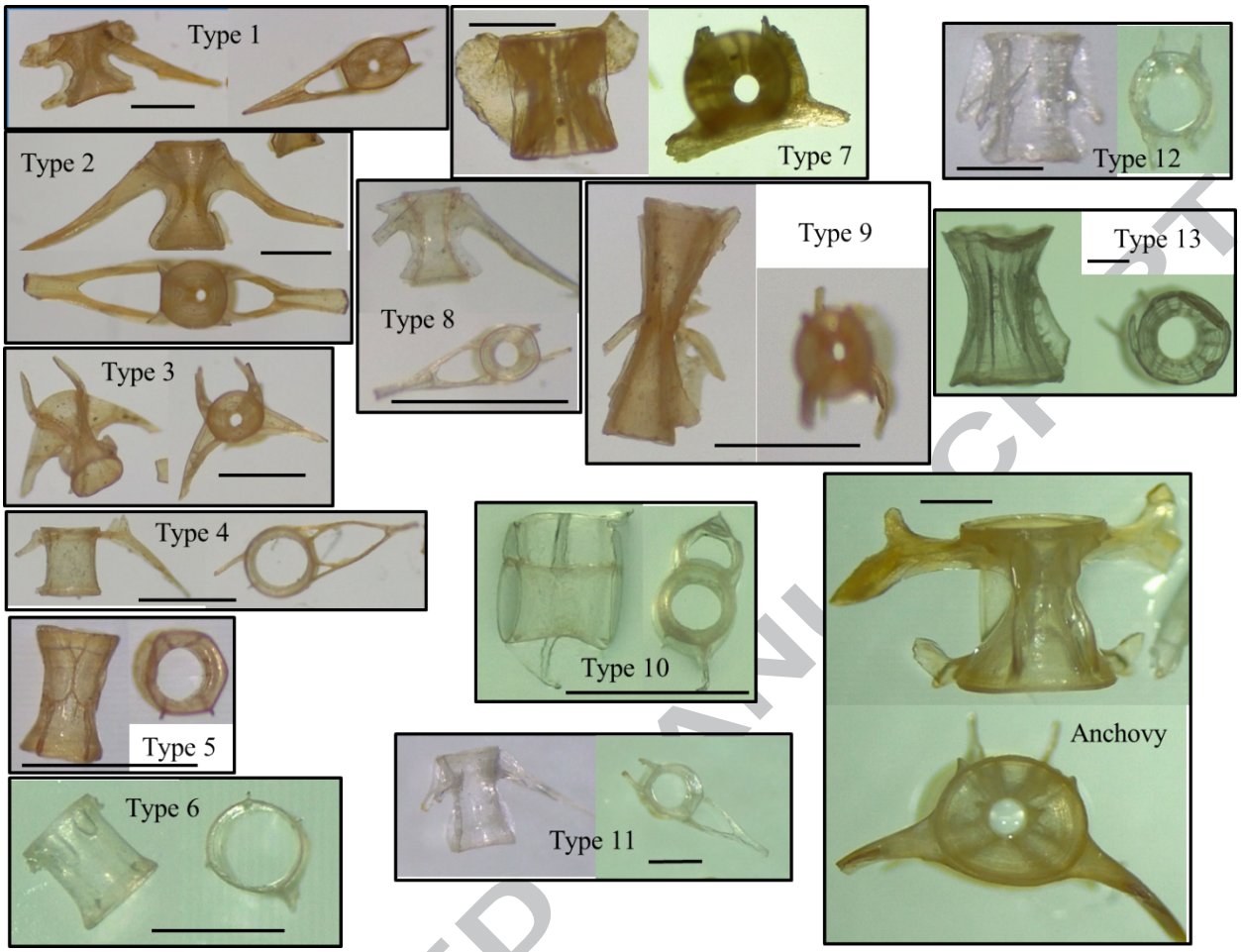

Figure 5. Different types of non-identified vertebrae found in the composite core B14-G10-G14. A picture of an anchovy vertebrae is also shown for comparison. Scale bar represents 1 mm. The vertebrae type 5 corresponds to *Vincinguerria lucetia* (compare and contrast type 5 image and the vertebrae located at the bottom right side of Figure 3H), the types 11 and 12 might also correspond to *Vincinguerria lucetia* and the type 13 could correspond to a myctophid according to the findings of Rose (2013).

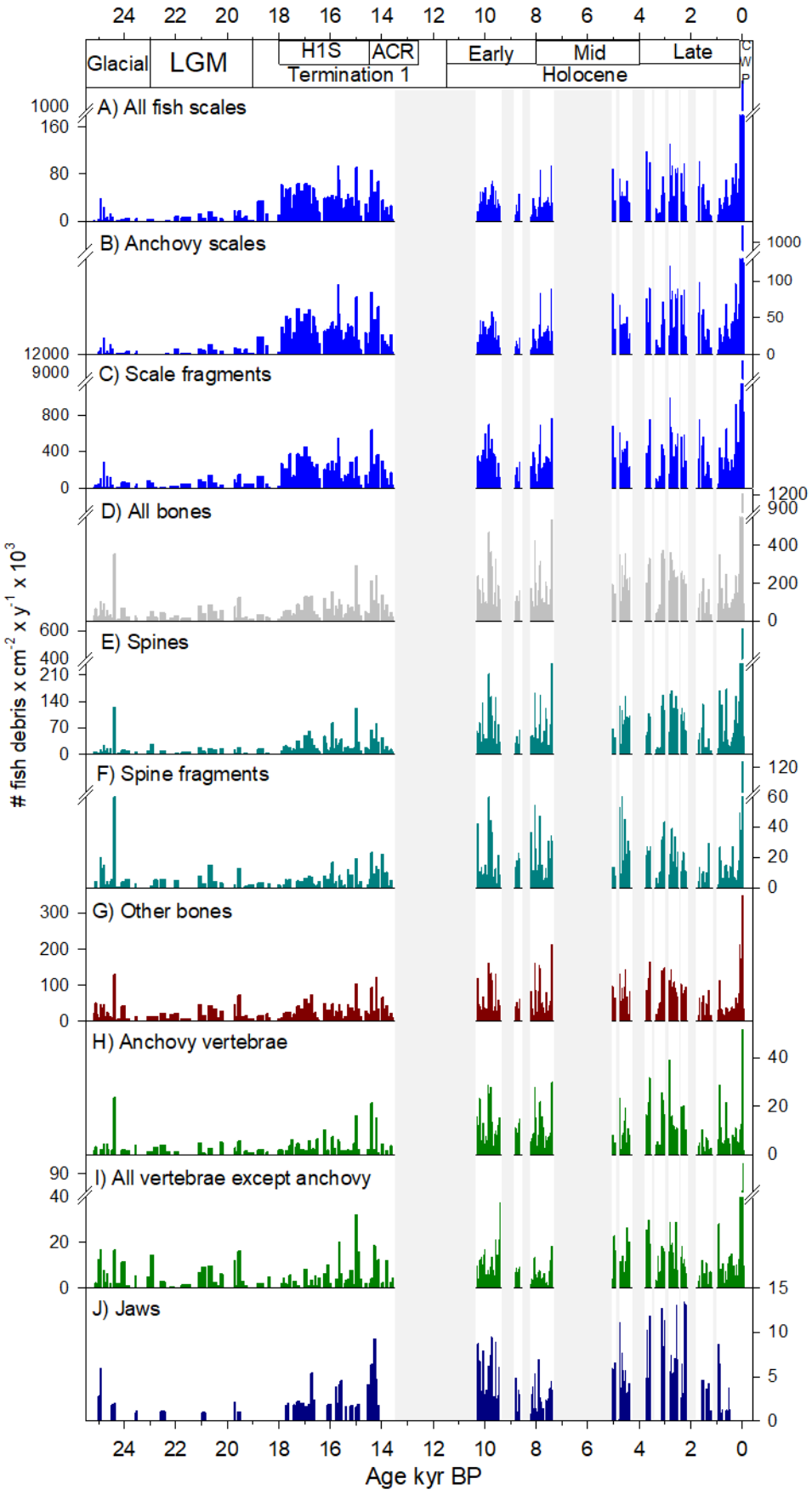

Figure 6. Fish debris fluxes in the composite record B14-G10-G14. A) All fish scales. B) Anchovy scales. C) Scale fragments. D) All bones. E) Spine. F) Spine fragments. G) Other bones. H) Anchovy vertebrae. I) All vertebrae except anchovy. J) Jaw bones. In core B-14, jaw bones were quantified as bones. The acronyms used in this figure as follow: Last Glacial Maximum (LGM), Heinrich 1 Stadial (H1S) and Antarctic Cold Reversal (ACR). The shaded gray areas indicate samples associated with homogeneous or slumped deposits where fish scales were not analyzed and also the time period not covered by G-10 and G-14 between the Termination 1 and the Holocene.

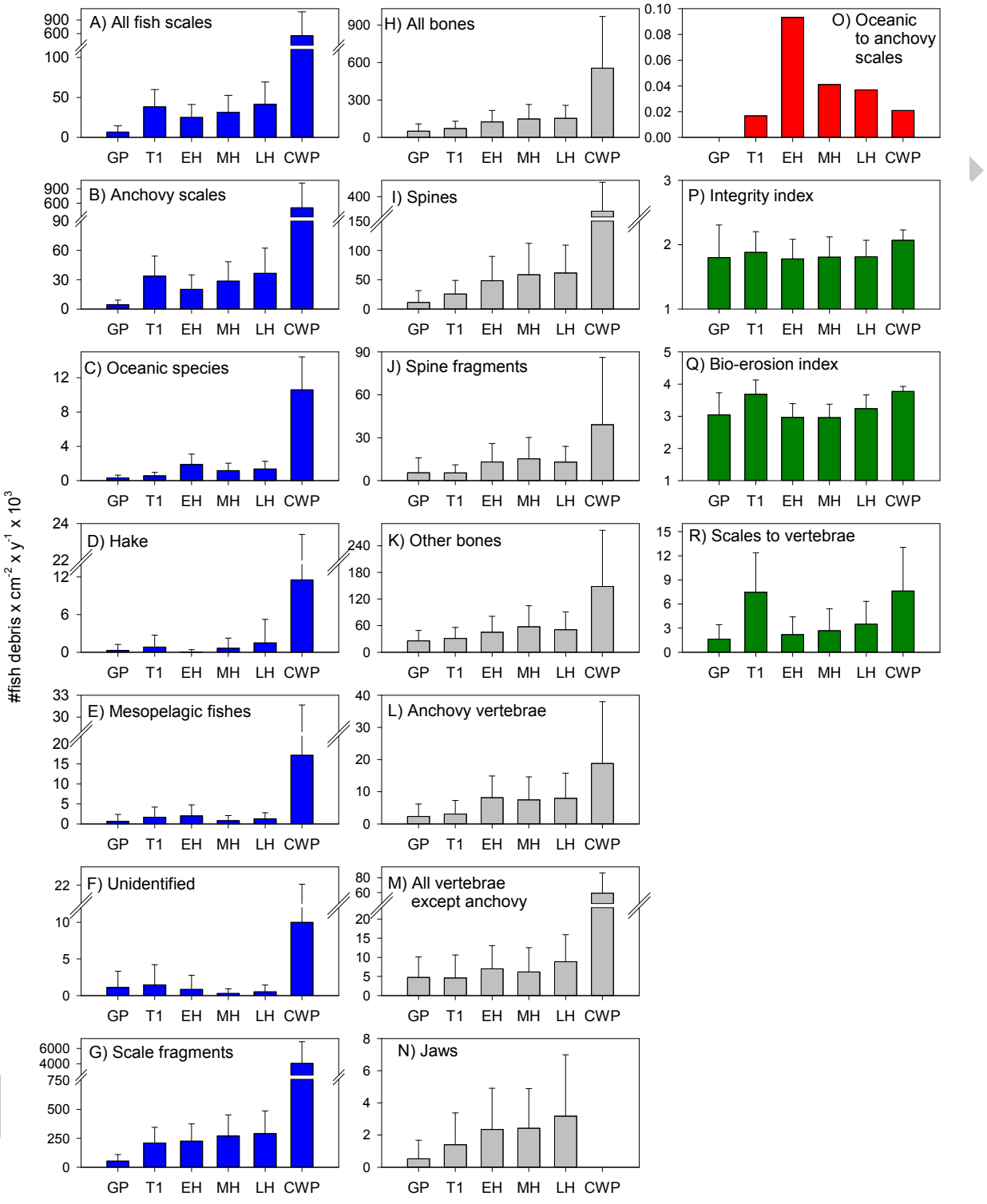

Figure 7. Average and standard deviation of the different types of fish debris fluxes lumped in periods of interest. A) All fish scales fluxes. B) Anchovy scales fluxes. C) Oceanic species scales fluxes, which includes the fish scales of sardine, jack mackerel, chub mackerel and saury. D) Hake scales fluxes. E) Mesopelagic fish scales fluxes. F) Unidentified fish scales fluxes. G) Scale fragments fluxes. H) Fluxes of

all bones, which includes the fluxes of spines, spine fragments, other bones, anchovy vertebrae and other vertebrae. I) Spine fluxes. J) Spine fragments fluxes. K) Other bones fluxes. L) Anchovy vertebrae fluxes. M) Fluxes of all vertebrae except anchovy. N) Jaw bones fluxes. O) Ratio of the fish scales from oceanic species to anchovy, this ratio was calculated by dividing the accumulated sardine, jack mackerel, chub mackerel and saury fluxes to the anchovy fluxes. P) Integrity index. Q) Bio-erosion index. R) Ratio of fish scales to vertebrae from all species. The acronyms used in this figure are: Current Warm Period (CWP), Late Holocene (LH), Mid-Holocene (MH), Early Holocene (EH), Termination 1 (T1), and Glacial period (GP) which includes the Glacial and Last Glacial Maximum periods from Figure 6.

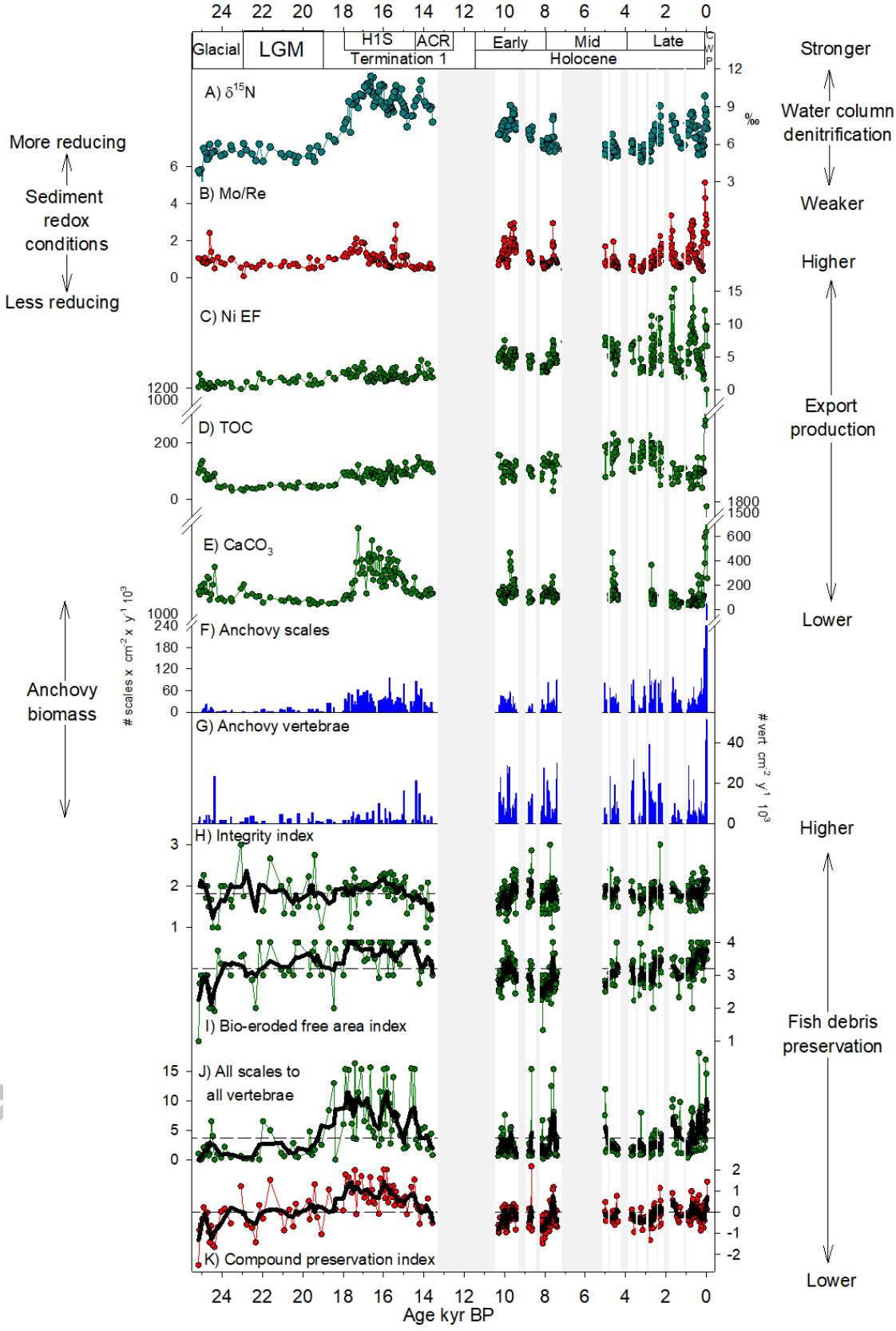

Figure 8. Comparison of the anchovy scales and vertebrae fluxes with proxies for environmental conditions and fish debris preservation. A) $\delta^{15}N$ as a proxy for water column denitrification and hence sub-surface deoxygenation. B) Mo/Re ratio, higher values indicate more reducing conditions in the sediment. C) Ni EF, as a proxy for export production. D) TOC fluxes, as a proxy for export production. E) Calcium carbonate as a proxy for export production. F) Anchovy scale fluxes. G) Anchovy vertebrae fluxes. H) Integrity index. I) Bio-eroded free area index. J) Ratio of scales to vertebrae from all species. K) Compound preservation index. The thick black line in H, I, J and K represents a five-interval moving average. The shaded gray areas indicate samples associated with homogeneous or slumped deposits where fish scales were not analyzed, and the time period not covered by G-10 and G-14 between the Termination 1 and the Holocene.

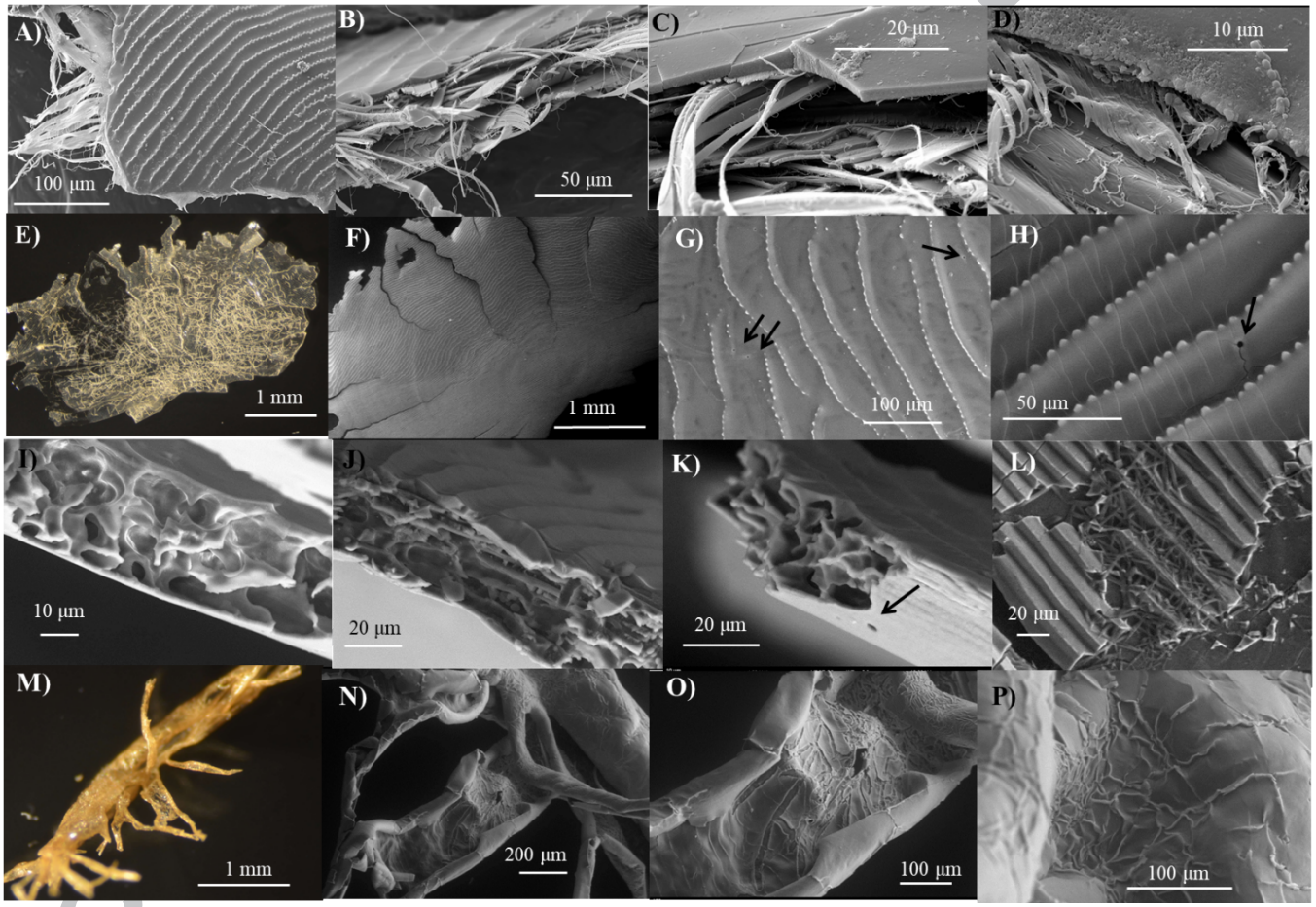

Figure 9. Scanning electron microscope (SEM) and conventional images of fresh and degraded anchovy scales. A) SEM image of a ripped portion of an anchovy scale taken from a recently caught fish. B) Vertical section of the same scale shown in A. C and D) zoom of the scale in A showing the collagen layers. E) Conventional image of an anchovy scale with tunnels dug by bio-eroders all over the scale. F) SEM image of the surface of the same anchovy scale in E without any evident sign of degradation over the scale. G) and H) Zoom of the anchovy scale shown in F, showing small holes over the scale surface (arrows). I, J and K) Vertical section of the anchovy scale in E showing the multiple channels dug by bio-eroders. Image show in K also presents a hole over its surface (black arrow). L) Close-up image of another anchovy scale that present loss of the surface layer and needle-type formations. M) Conventional photograph of a flimsy and rolled-up anchovy scale. N, O and P SEM images of the same anchovy scale in M.

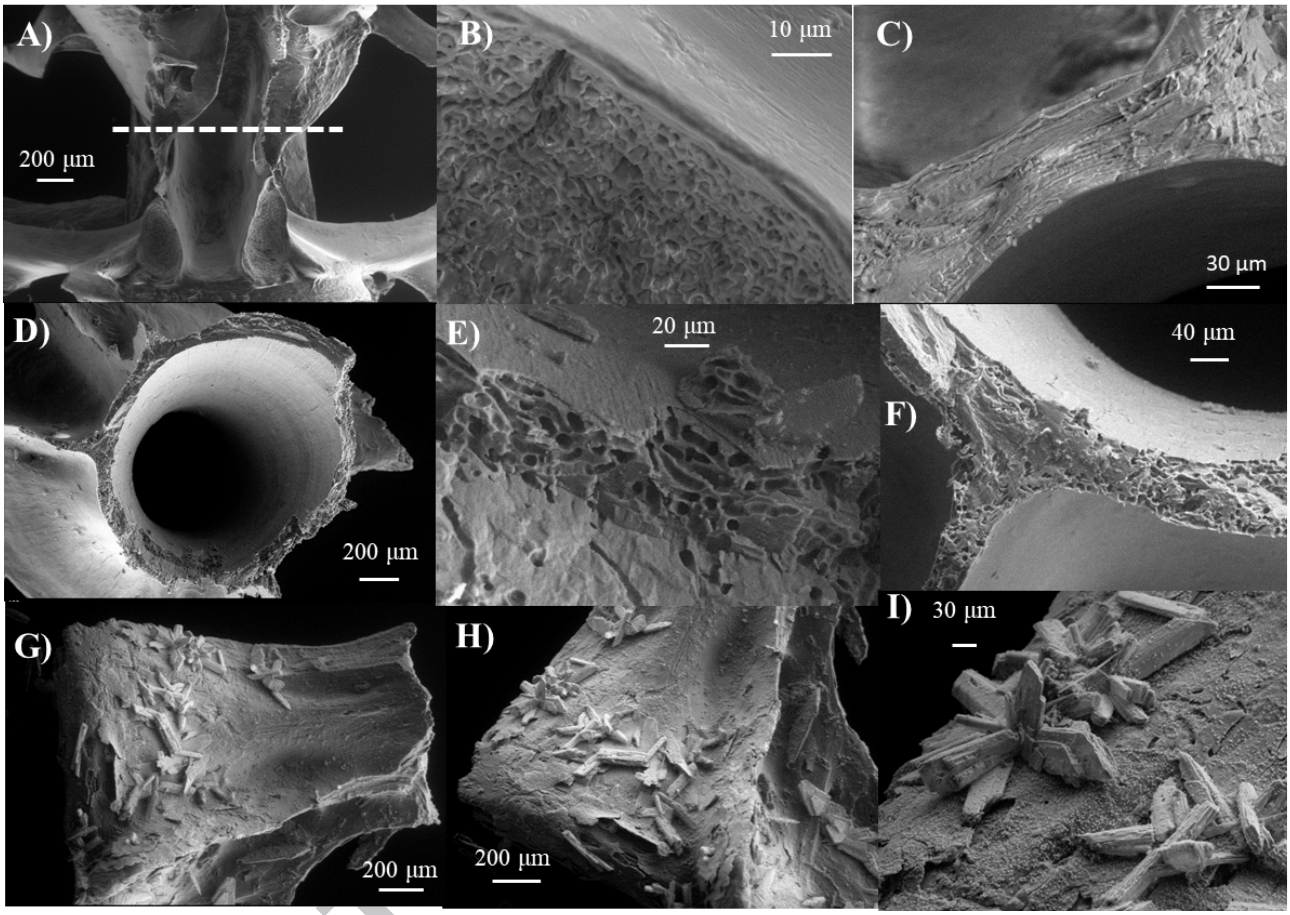

Figure 10**.** Scanning Electron Microscope (SEM) images of anchovy (*Engraulis ringens*) vertebrae from a recently caught individual (A to C), with strong signs of bio-erosion (D to F), and with mineral crystals over the vertebrae surface (G to I). A) SEM image of an anchovy vertebrae, the discontinuous line indicates the position were the vertebrae was cut to observe the internal components. B) Detail of the oval structure where the dorsal spines are attached to the vertebra. C) Vertical sections of the vertebrae shown in A.D) Vertebrae with strong evidence of bio-erosion. E) Zoom of the vertebrae shown in D) showing the galleries done by bio-eroders. F) Vertical section of the vertebrae in D) showing also the presence of galleries (compare and contrast D with F). G) Vertebra found in sample G14 S1B 45 from the LGM showing the presence of minerals over the surface. H) Zoom of the same vertebra shown in G). I) Zoom of the vertebrae in I showing the unidentified minerals.

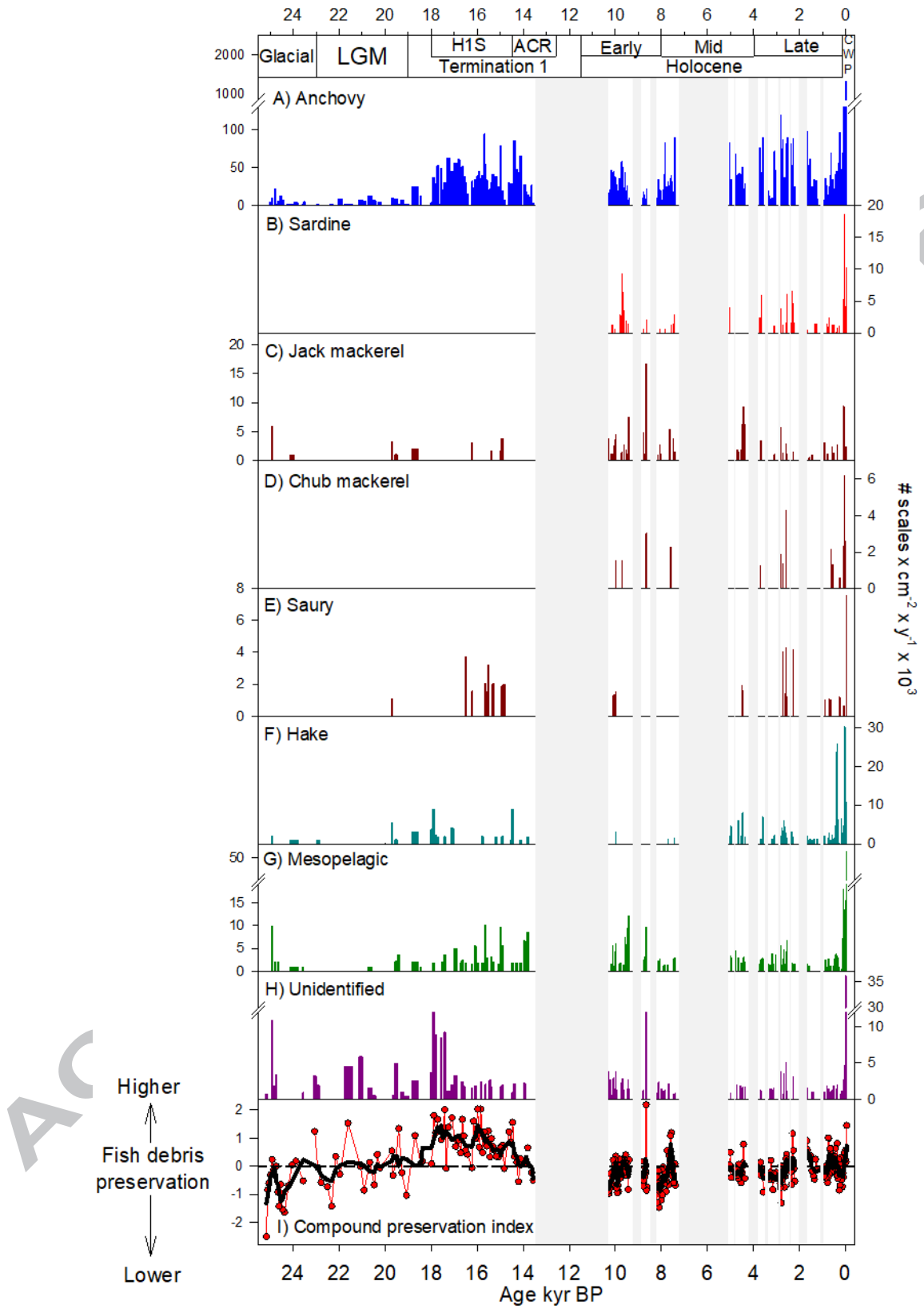

Figure 11. Detailed fish scale fluxes composition. A) Anchovy (*Engraulis ringens*). B) Sardine (*Sardinops sagax sagax*). C) Jack mackerel (*Trachurus picturatus murphyi*). D) Chub mackerel (*Scomber*

japonicus). E) Saury (*Scomberesox saurus scombroides*). F) Hake (*Merluccius gayi peruanus*). G) Mesopelagic fishes. H) Non-identified species. I) Compound preservation index, the thick black line represents a five-interval moving average. The shaded gray areas indicate samples associated with homogeneous or slumped deposits where fish scales were not analyzed and also the time period not covered by G-10 and G-14 between the Termination 1 and the Holocene.

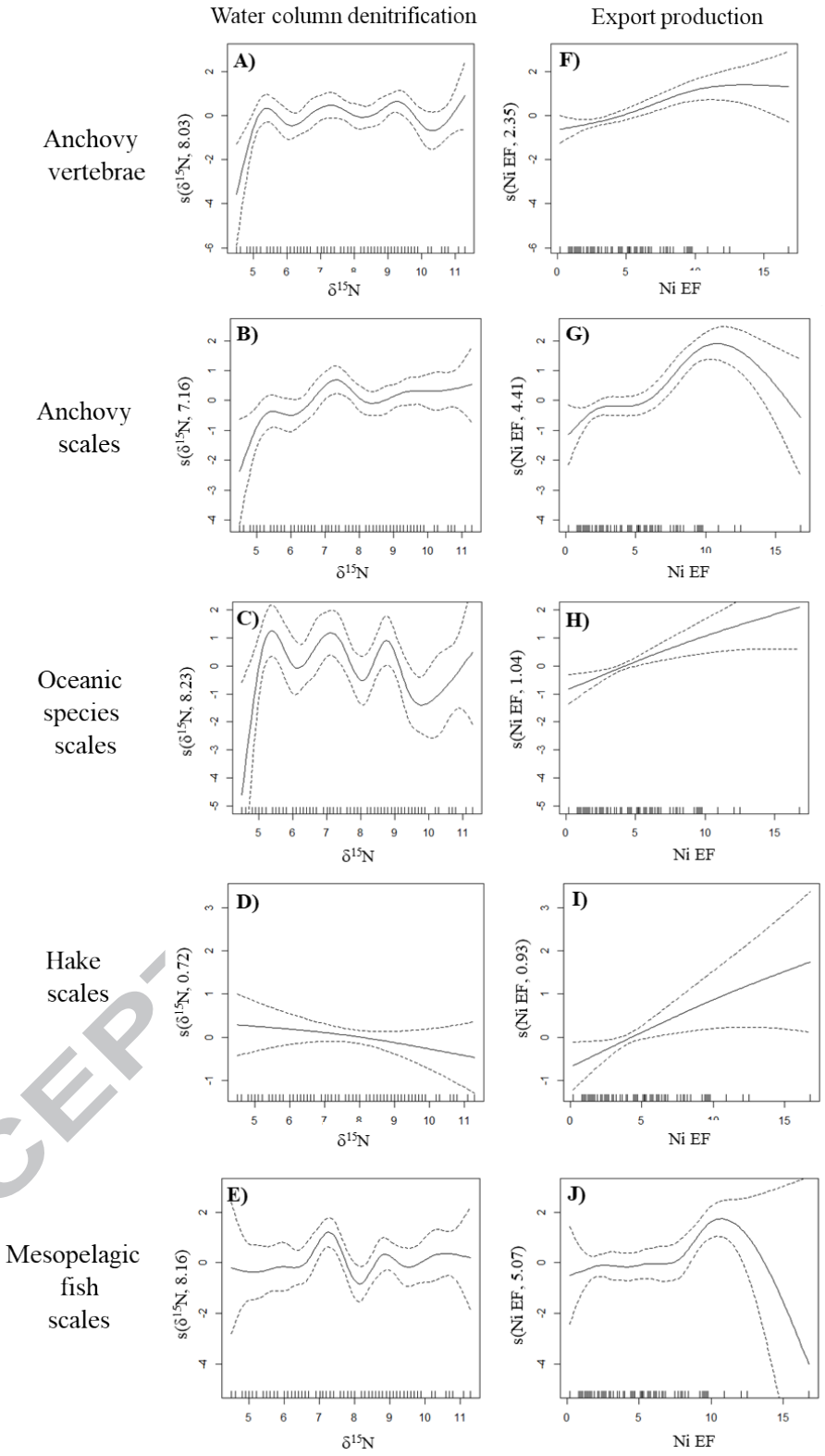

Figure 12. Generalized additive models (GAMs) between fish debris fluxes and proxies for water column denitrification ($\delta^{15}N$) and export production (Ni EF). A) $\delta^{15}N$ versus anchovy vertebrae. B) $\delta^{15}N$ versus anchovy scales. C) $\delta^{15}N$ versus oceanic species scales, which includes sardine, jack mackerel, chub

mackerel and saury. D) $\delta^{15}N$ versus hake scales. E) $\delta^{15}N$ versus Mesopelagic species. F) Ni EF versus anchovy vertebrae. G) Ni EF vs anchovy scales. H) Ni EF versus oceanic species scales. I) Ni EF versus hake scales. J) Ni EF versus Mesopelagic fish scales. The intervals selected for this analysis were the samples ($\delta^{15}N$ n=112; Ni EF n=135) characterized by good fish scale preservation (i.e. values of the compound preservation index higher than zero, see Fig. 8K), Tick marks on the x-axis represent observed data points. Y-axis represents the smooth fitted function of the dependent values and are centered to zero. The values in parentheses in the y-axis label indicate the degree of freedom of the model.

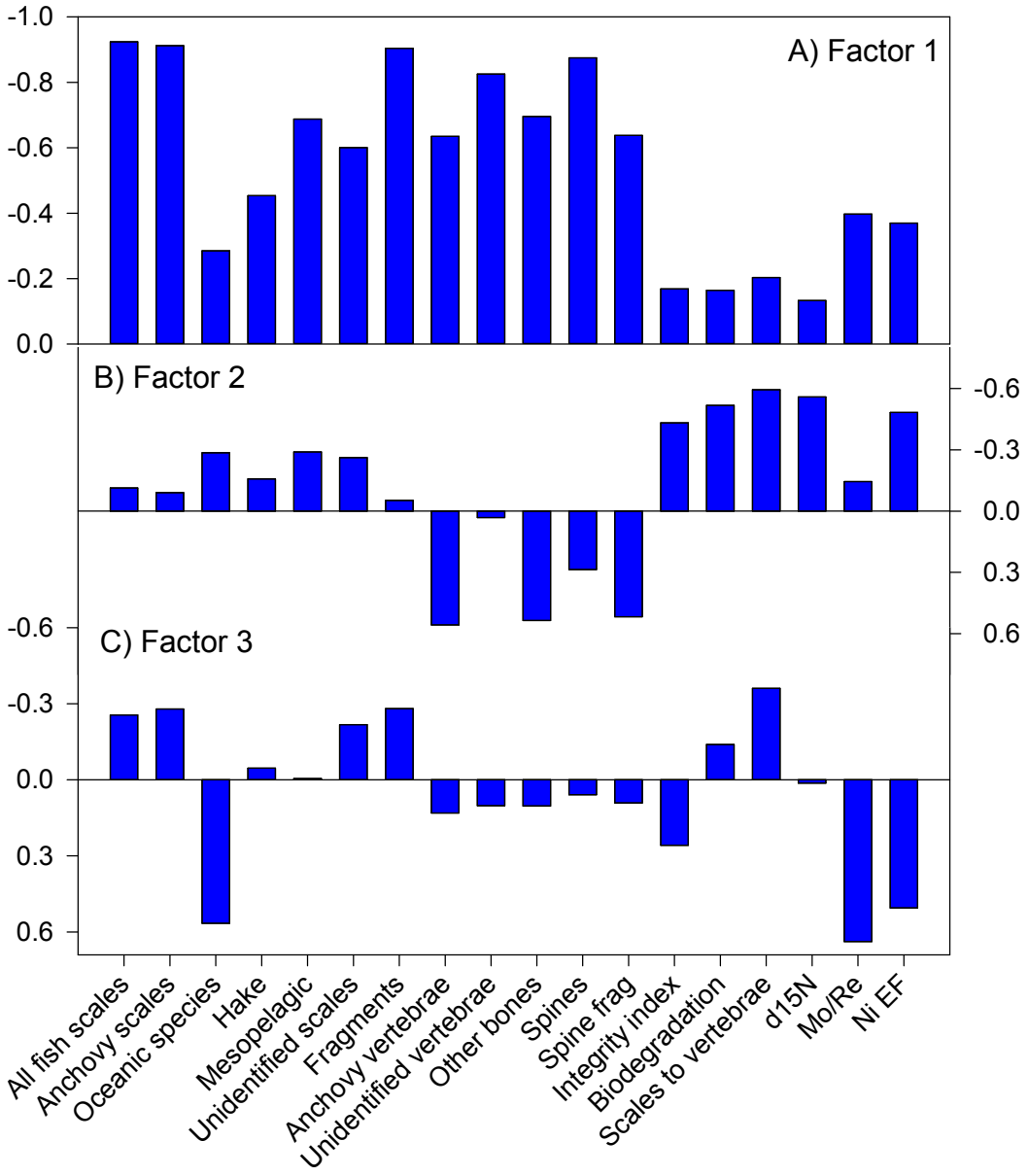

Figure 13. Loadings of the 3 main principal components of the 19 selected variables. The PC1, PC2 and PC3 explain 40.1, 13.9 and 8.3% of the data set variance.

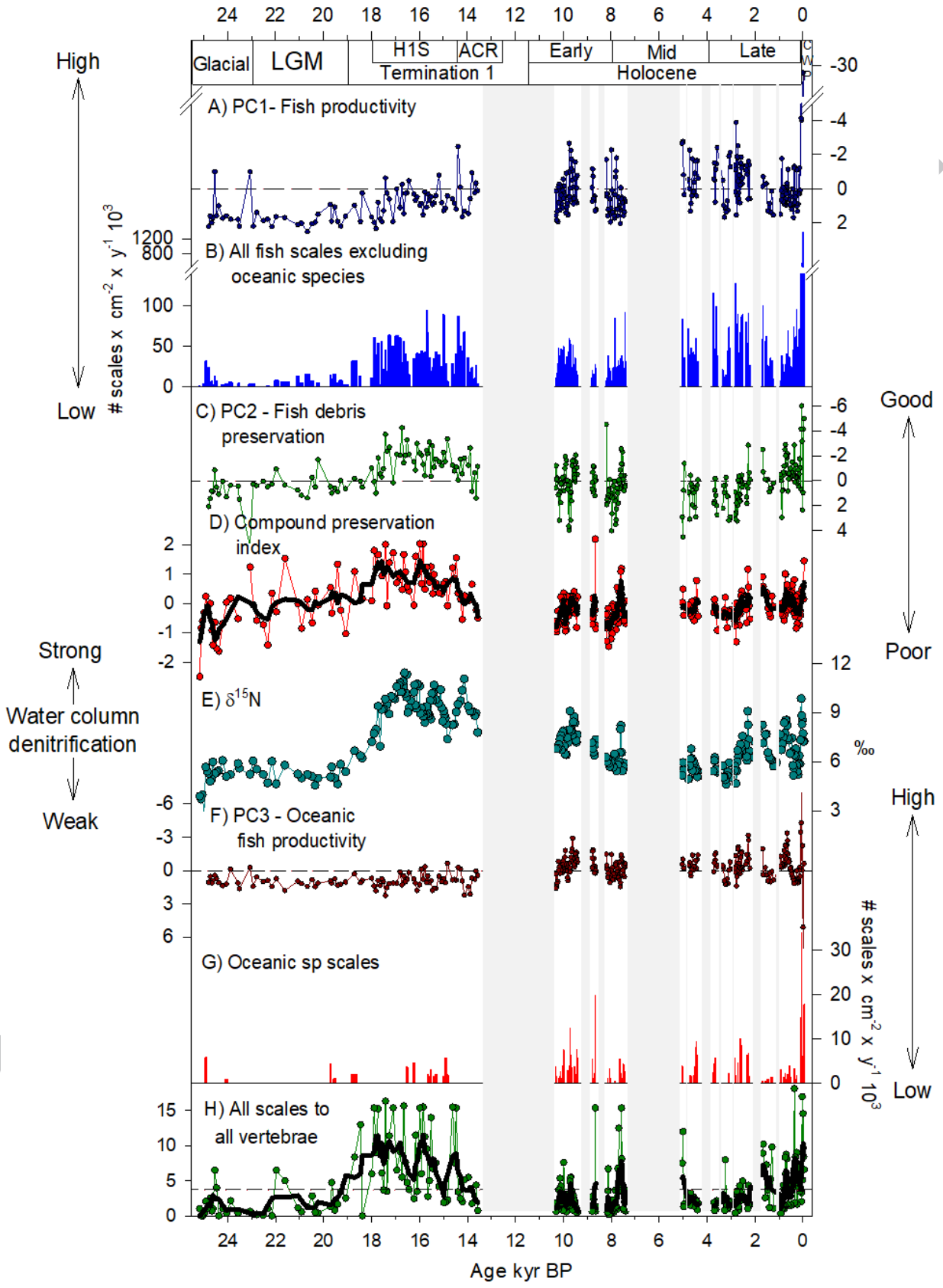

Figure 14. Time series of the main 3 principal components. A) PC1 representing the fish production excluding the oceanic fishes. B) Fluxes of all fish species and groups excluding the oceanic species. C) PC2 representing the preservation signal. D) Compound preservation index as shown in Fig. 8K. E) $\delta^{15}N$ as a proxy for water column denitrification and hence sub-surface deoxygenation as shown in Fig. 8A. F) PC3 representing the fish production of oceanic species and its impact on the fluxes of fish bones to the sediment. G) Fluxes of oceanic species (sardine, jack mackerel, chub mackerel and saury). H) Ratio of all scales to all vertebrae as shown in Fig. 8J.

Highlights

- Anchovy and other fishes fluctuated from multidecadal to millennial timescales
- Productivity appears as the main factor controlling small pelagic fish abundance
- Sub-surface oxygenation seems to play a role in a species-dependent way
- The industrial fishery developed during a period of exceptional fish productivity